Mechanics of Advanced Materials and Structures
Publication details, including instructions for authors and subscription information:
http://www.tandfonline.com/loi/umcm20

An Introduction to a Compatible Spectral Discretization Method

Marc Gerritsma [a]

[a] Department of Aerospace Engineering, Delft University of Technology, Kluyverweg 1, 2629 HS, Delft, The Netherlands

Accepted author version posted online: 14 Mar 2012.Published online: 21 Mar 2012.

To cite this article: Marc Gerritsma (2012) An Introduction to a Compatible Spectral Discretization Method, Mechanics of Advanced Materials and Structures, 19:1-3, 48-67, DOI: 10.1080/15376494.2011.572237

To link to this article: http://dx.doi.org/10.1080/15376494.2011.572237

Mechanics of Advanced Materials and Structures, 19:48–67, 2012

ISSN: 1537-6494 print / 1537-6532 online
DOI: 10.1080/15376494.2012.572237

Taylor & Francis
Taylor & Francis Group

An Introduction to a Compatible Spectral Discretization Method

Marc Gerritsma
Department of Aerospace Engineering, Delft University of Technology, Delft, The Netherlands

In this article, I try to explain what one means when one refers to 'compatible' or 'mimetic' discretization methods. I will show why this approach is so appealing from a computational and physical point of view. In this respect, this is not really a scientific paper, although some new ideas will be presented, but—as the title suggests—an *introduction* to a new way of looking at discretization methods. This article shows the path from physical modeling, to a representation in terms of differential forms, algebraic topological cochains with an implementation in terms of an orthogonal polynomial.

Keywords spectral element method, differential geometry, algebraic topology, finite element method, finite volume method

1. INTRODUCTION

Before I invite you to start on this exposé on so-called *compatible* or *mimetic* discretization methods, I need to point out briefly what these types of numerical schemes are. Basically, compatible or mimetic schemes are numerical schemes that *mimic* the continuous differential equation as much as possible. This means that our primary interest is not to minimize the truncation error or the residual in any sense; a brute-force approach that has been the cornerstone of computational science in the last 40 years. Instead, we will take a closer look at what the variables in our differential model actually mean.

Although we usually write $u(x, y, z, t)$ for a displacement or velocity at position (x, y, z) at time t, this description has lost one of the most important characteristics: its *geometric content*. Physical variables do not wander around aimlessly in space and time, but are associated to geometric objects. In this article, we will review where and how we lost this geometric content and demonstrate why it is so important to re-establish the connection with the underlying geometry. Simple examples will illustrate why it is important to consider the associated geometry. In vector calculus, we distinguish between scalar variables and vector variables, but not all scalars and vectors are the same. Consider, for instance, a temperature field, $T(x, y, z)$, a scalar quantity, which is defined at each point and the density, $\rho(x, y, z)$, which is associated with a volume. Both variables are represented by a scalar field, but one refers to point values (the temperature) and the other to the average mass per volume (density). The same holds for vectors where it is not always clear to which geometric objects the quantities are associated. Consider, for instance, a potential flow $\boldsymbol{u}(x, y, z) = \mathbf{grad}\,\phi$ that is defined along line segments or contours and the flux vector $\boldsymbol{f}(x, y, z)$ that is defined with respect to surfaces. In both cases, the quantities are described by vectors, but one refers to an object associated along lines (the velocity field) and the other to surfaces (the flux).

These examples illustrate that traditional vector calculus is inadequate to give a full representation of the physical variable and its relation to the geometry. We will, therefore, introduce in this article an alternative way to represent variables and differential equations: differential geometry. In terms of differential geometry we write $T^{(0)}$, indicating that T is associated with zero-dimensional objects (points) and $\rho^{(3)}$ which shows that the density is associated with three-dimensional objects (volumes). Similarly, we write $u^{(1)}$ and $f^{(2)}$ to distinguish between vectors acting along one-dimensional objects (lines) and vectors associated with two-dimensional objects (surfaces). In this case, there is no need to print u and f in bold face, because it will be clear from the context that we deal with a vector quantity. There are several other reasons to introduce differential geometry as the preferred language for physical models. One reason is that the vector operations **grad** , **curl** , and **div** are all represented by one operator in differential geometry: the exterior derivative, d. And the other reason to use differential geometry is that many concepts from differential geometry have a natural discrete representation: in terms of algebraic topology. The exterior derivative, just mentioned, is naturally represented by the so-called coboundary operator, δ. Due to this—almost—one-to-one correspondence between the continuous differential form and the discrete algebraic topological form, discretization of differential equations is almost like a translation using a (mathematical) dictionary: Replace every continuous form by its natural discrete form.

Received 14 August 2009; accepted 31 January 2011.
Adderess correspondence to Marc Gerritsma, Department of Aerospace Engineering, Delft University of Technology, Kluyverweg 1, 2629 HS Delft, The Netherlands. E-mail: M.I.Gerritsma@TUDelft.nl

Unfortunately, this is not completely true. Not all continuous relations have a natural discrete counterpart and this is where the actual numerical modeling needs to be invoked. Some of you may opt for finite difference approximations, whereas others decide to use finite element methods. What do we gain by this mimetic approach, if in the end we still need to use classical techniques? Well, bear in mind that only a small part of the original differential equation needs to be approximated by conventional numerical techniques. In fact, the part that has a natural discrete representation will in fact be exact and metric free.

If we look more closely at what the variables in our differential model mean, we can develop numerical schemes that obey certain characteristics or symmetries from the outset. Many of these symmetries are purely topological, meaning independent of lengths and angles. This implies that we can encode these symmetries numerically on any type of grid; it should give the same result on coarse meshes as on fine meshes and the symmetries should be satisfied on nice orthogonal grids and highly skewed—even self-overlapping—grids.

Although many of the concepts described in this article may be new to some people, there is quite some literature available. As far as I know, Enzo Tonti [1], was the first to classify physical theories on a geometric basis. Mattiussi [2], in 2000 wrote a very lucid overview on the geometric methods and also describes the connection with various established numerical techniques. Another reference that greatly influenced this article was written by Alain Bossavit and on his website he refers to these papers as the "Japenese papers" [3]. In the finite difference world, one should mention Mikhail Shashkov, Stanly Steinberg, Nicolas Robidoux, and Mac Hyman [4–7], where symmetry considerations on irregular grids play a central role [8–10]. Also, in a finite difference setting is the paper by Robidoux and Steinberg, [11], which relies heavily on geometric considerations. Bochev [12], in a Von Karman Institute lecture gives an overview of mixed Galerkin methods, least-squares formulations, and geometric methods. Bochev and Hyman [13] describe geometric methods and propose the reduction and reconstruction operators to be discussed in this article. Arnold, Falk, and Winther [14, 15] have set up a very comprehensive finite elements exterior calculus framework. Brezzi and Buffa [16] endorse the use of cochains in solving electromagnetic problems. Hiptmair [17] and Tarhasaari et al. [18] show that mass-matrices in finite element methods play the role of Hodge matrices in a finite element setting. Perot [19–21] has applied mimetic structures to finite volume methods for unstructured meshes. A pure geometrical setting in which the use of interpolation is avoided as much as possible is given by Desbrun and co-workers [22,23]. This list is by no means exhaustive, but for those who are interested in the subject these references may prove to be a good introduction.

A novel feature in this article is that I will introduce mimetic methods on quadrilaterals, where in many papers only triangular elements are discussed. The special basis functions that will be introduced in this article are, if I am correct, the extension of the classical Whitney forms to quadrilaterals. Since I am not sure whether this is really the case, I have chosen to call them *edge functions*.

The outline of this article is as follows: In section 2, we review how we model a conservation law and how we lose any connection with the underlying geometry when we move from an integral formulation to a differential formulation. In section 3, I introduce some concepts from differential geometry that we will need to get a differential formulation that still contains the geometric information. In section 4, the basic ingredients from algebraic topology will be given to be used subsequently in section 5, where higher order cochain interpolations are introduced. Final remarks are given in section 6.

2. DIFFERENTIAL MODELING

In order to show how we use geometric aspects when we set up physical models, let us look at conservation of mass. The derivation of this conservation law follows the one given by Anderson Jr. [24]. Consider any arbitrary, fixed volume $\mathcal{V} \in \mathbb{R}^3$ with boundary $\partial\mathcal{V}$. An engineering derivation of conservation of mass then proceeds by saying: Let's consider a small volume, $d\mathcal{V}_i \subset \mathcal{V}$, which is small enough, such that the density within this volume can assumed to be constant. So the mass contained in $d\mathcal{V}_i$ is equal to $\rho_i\, d\mathcal{V}_i$. If we assume that the volume $\mathcal{V}$ is covered by such non-overlapping small volumes $d\mathcal{V}_i$, then the total mass in $\mathcal{V}$ is given by

$$\sum_i \rho d\mathcal{V}_i \quad \longrightarrow \quad \int_{\mathcal{V}} \rho\, d\mathcal{V}. \tag{1}$$

So the mass contained in $\mathcal{V}$ is defined in terms of Riemann integrals. Now the principle of conservation of mass states that mass can neither be created nor destroyed. So, if the total amount of mass inside $\mathcal{V}$ changes as a function of time, then this must be due to a mass-influx through the boundary $\partial\mathcal{V}$. Now, if we consider a small surface element $\partial\mathcal{V}_i \subset \partial\mathcal{V}$, which we assume small enough such that the normal velocity, $\mathbf{u}_i$ and the density ρ_i through $\partial\mathcal{V}_i$ are constant in the time interval Δt, then the amount of mass flowing through $\partial\mathcal{V}_i$ between t and $t + \Delta t$ *out* of the volume $\mathcal{V}$, is given by

$$\rho_i(t)\mathbf{u}_i \cdot \mathbf{n}_i dS_i \cdot \Delta t, \tag{2}$$

in which $\mathbf{n}_i$ is the outward unit normal to $\partial\mathcal{V}_i$ and dS_i denotes the area of the little surface element, $\partial\mathcal{V}_i$. The net outflux through the boundary of $\mathcal{V}$ is given by

$$\sum_i \rho_i \mathbf{u}_i \cdot \mathbf{n}_i\, dS_i \cdot \Delta t \quad \longrightarrow \quad \Delta t \int_{\partial\mathcal{V}} \rho\mathbf{u} \cdot \mathbf{n}\, dS. \tag{3}$$

So if we invoke the principle of conservation of mass, we see that the time-rate of change of mass inside $\mathcal{V}$ plus the net outflux

of mass through the boundary must be equal to zero:

$$\int_{\mathcal{V}} \rho(t+\Delta t)\, d\mathcal{V} - \int_{\mathcal{V}} \rho(t)\, d\mathcal{V} + \Delta t \int_{\partial\mathcal{V}} \rho \mathbf{u}\cdot\mathbf{n}\, dS = 0. \quad (4)$$

This integral statement of conservation of mass is the starting point for finite volume methods. Similar derivations can be given for other conservation laws, such as conservation of momentum, energy, circulation in potential flows, etc., see [24]. The reason why this small derivation is given, is to exemplify that in many (if not all) physical descriptions the geometry plays an important role. In the above example, we worked with an arbitrary volume $\mathcal{V}$, its boundary $\partial\mathcal{V}$, two time instants, t and $t+\Delta t$, and a time interval Δt as the main geometric building blocks.

Let us now look how we can rewrite the conservation law in differential form. By dividing (4) by Δt and taking the limit $\Delta t \to 0$, the first two terms can be written as

$$\lim_{\Delta t\to 0} \frac{d}{dt} \int_{\mathcal{V}} \frac{\rho(t+\Delta t)-\rho(t)}{\Delta t}\, d\mathcal{V} = \int_{\mathcal{V}} \frac{\partial \rho}{\partial t}\, d\mathcal{V}. \quad (5)$$

Secondly, the boundary integral can be rewritten as a volume integral using the divergence theorem

$$\int_{\partial\mathcal{V}} \rho\mathbf{u}\cdot\mathbf{n}\, dS = \int_{\mathcal{V}} \mathbf{div}\ (\rho\mathbf{u})\ d\mathcal{V}. \quad (6)$$

So the integral formulation is then given by

$$\int_{\mathcal{V}} \frac{\partial \rho}{\partial t}\, d\mathcal{V} + \int_{\mathcal{V}} \mathbf{div}\ (\rho\mathbf{u})\ d\mathcal{V} = \int_{\mathcal{V}} \left[\frac{\partial \rho}{\partial t} + \mathbf{div}\ (\rho\mathbf{u})\right] d\mathcal{V} = 0. \quad (7)$$

This integral identity must hold for each arbitrary volume $\mathcal{V}$, which implies that

$$\frac{\partial \rho}{\partial t} + \mathbf{div}\ (\rho\mathbf{u}) = 0. \quad (8)$$

Here, we have the familiar differential form that generally is the starting point for finite difference methods and finite element methods. Note that in passing from the integral form to the differential form the direct correspondence with geometric quantities is lost. The density is a scalar quantity, but it is not clear anymore that this scalar is associated with volumes. The flux $\mathbf{f} = \rho\mathbf{u}$ is a vector, but in the differential formulation it is not apparent that this vector acts on surfaces.

Although the equations (4) and (8) are completely equivalent, numerical methods based on (4) (finite volume methods) generally have different properties than methods based on (8) (finite difference methods, finite element methods). This can be partly attributed to the fact that one chooses a discrete setting in which the role of the geometry is ignored. Note that in passing from the integral formulation to the differential form, the divergence theorem is an essential step. The mimetic method that will be discussed in this article takes the divergence theorem (and other integral theorems) as the starting point on which the discrete setting is based. The resulting scheme, therefore, is somewhere between finite volume and finite element methods.

Before I move on to a differential formulation, which still contains the—what I will call—geometric content, it is worth noting that the divergence operator introduced in (6) takes quantities defined on a surface and maps it on to quantities defined on volumes. Following Robidoux and Steinberg [11], we can write

$$H_S \xrightarrow{\ \mathbf{div}\ } H_V, \quad (9)$$

where H_S is the space of variables defined on surfaces and H_V the space of variables defined in volumes. So the divergence operator converts variables with different geometric content. The vector operators **grad** and **curl** do a similar thing. This can be seen by looking at the integral theorems associated with these operators. For **grad**, for instance, we have for an arbitrary curve $\mathcal{C}$ connecting the points P_1 and P_2

$$\int_{\mathcal{C}} \mathbf{grad}\,\phi\cdot d\mathbf{s} = \phi(P_2) - \phi(P_1). \quad (10)$$

Here ϕ is a scalar function which acts on points, otherwise the right-hand side wouldn't make sense. **grad** ϕ, on the other hand, is defined along any curve and it therefore associated with line segments. So the gradient operator maps variables defined in points to variables defined along line segments. Again, using the suggestive notation of Robidoux and Steinberg [11], this can be denoted as

$$H_P \xrightarrow{\ \mathbf{grad}\ } H_L, \quad (11)$$

where H_P is the space of quantities defined in points and H_L is the space of physical quantities defined along line segments. The curl operator, finally, maps quantities defined along line segments to quantities defined on surfaces. This is reflected in the classical Stokes theorem: Let $\mathcal{S}$ be an arbitrary surface enclosed by $\mathcal{C} = \partial\mathcal{S}$, then

$$\int_{\mathcal{C}} \mathbf{a}\cdot d\mathbf{s} = \int_{\mathcal{S}} \mathbf{curl}\,\mathbf{a}\cdot dS. \quad (12)$$

This leads to

$$H_L \xrightarrow{\ \mathbf{curl}\ } H_S. \quad (13)$$

So the three vector operators provide the following sequence

$$H_P \xrightarrow{\ \mathbf{grad}\ } H_L \xrightarrow{\ \mathbf{curl}\ } H_S \xrightarrow{\ \mathbf{div}\ } H_V. \quad (14)$$

This sequence is exact in the sense that the range of one of these operators is contained in the null space of the next operator, i.e.,

$$\mathcal{R}(\mathbf{grad}) \subset \mathcal{N}(\mathbf{curl}) \quad \text{and} \quad \mathcal{R}(\mathbf{curl}) \subset \mathcal{N}(\mathbf{div}). \tag{15}$$

On connected and contractible domains, we even have equality:

$$\mathcal{R}(\mathbf{grad}) = \mathcal{N}(\mathbf{curl}) \quad \text{and} \quad \mathcal{R}(\mathbf{curl}) = \mathcal{N}(\mathbf{div}). \tag{16}$$

Such an exact sequence is called a De Rham complex and is usually given by

$$\mathbb{R} \longrightarrow H_P \overset{\mathbf{grad}}{\longrightarrow} H_L \overset{\mathbf{curl}}{\longrightarrow} H_S \overset{\mathbf{div}}{\longrightarrow} H_V \longrightarrow 0, \tag{17}$$

where $\mathbb{R}$ at the beginning of the sequence denotes the real constants that comprise the null space of the gradient and the 0 at the end of the sequence indicates that any other differential operator maps quantities onto 0, because in $\mathbb{R}^3$ there is no next operator. Note that in vector calculus quantities in H_P and H_V are given by scalar fields and quantities defined on H_L and H_S by vector fields. In finite element methods, the spaces H_P, H_L, H_S, and H_V are generally associated with the functions spaces, $H^1(\Omega)$, $H(\text{curl}; \Omega)$, $H(\text{div}; \Omega)$, and $L^2(\Omega)$, respectively.

3. DIFFERENTIAL GEOMETRY

In the previous section, it was shown that classical vector calculus is inadequate to fully capture the geometric structure of a partial differential equation. We, therefore, introduce in this section some elementary concepts from differential geometry that allow us to rephrase differential equations in such a way that its geometric content is preserved.

The main building blocks in differential geometry are the *exterior differential forms* or *differential forms*. These forms can be introduced in many ways, but for engineering purposes it suffices to say that differential forms are the objects "that one finds underneath an integral sign" according to Flanders [25]. Other common definitions are that k-forms are anti-symmetric k-tensors acting on vectors in $[T_x\mathbb{R}^n]^k$ [26, 27] or differential forms can be introduced as linear functionals on multi-vectors [1, 31].

3.1. Differential Forms

Following Flanders' introduction, we have that in $\mathbb{R}^3$ a 1-form is given by an expression of the form

$$\lambda^{(1)} = A(x, y, z)\,dx + B(x, y, z)\,dy + C(x, y, z)\,dz, \tag{18}$$

where the superscript (1) indicates that this is a 1-form. A 1-form can be integrated over one-dimensional, smooth curves $\mathcal{C}$ to give

$$\int_{\mathcal{C}} \lambda^{(1)} = \int_{\mathcal{C}} A(x, y, z)\,dx + B(x, y, z)\,dy + C(x, y, z)\,dz. \tag{19}$$

Another way of writing this integral is to consider it as duality pairing between the 1-form and the geometric one-dimensional curve $\mathcal{C}$:

$$\langle \lambda^{(1)}, \mathcal{C} \rangle := \int_{\mathcal{C}} \lambda^{(1)}. \tag{20}$$

The coefficients $(A(x, y, z), B(x, y, z), C(x, y, z))$ form the so-called *vector proxy* of the 1-form. Classical vector calculus only works with these vector proxies and ignores the basis vectors dx, dy, and dz, which tell us that this vector is associated with one-dimensional objects.

A 2-form is given by an expression of the form

$$\eta^{(2)} = P(x, y, z)\,dydz + Q(x, y, z)\,dzdx + R(x, y, z)\,dxdy. \tag{21}$$

Here the superscript (2) refers to the fact that we are considering a 2-form. The vector proxy in this case is formed by the triplet $(P(x, y, z), Q(x, y, z), R(x, y, z))$. Although this also represents a vector in vector calculus the distinction between the 1-forms and 2-forms is lost. 2-Forms are the natural objects to integrate over two-dimensional manifolds or surfaces.

$$\int_{\mathcal{S}} \eta^{(2)} = \int_{\mathcal{S}} P(x, y, z)\,dydz + Q(x, y, z)\,dzdx + R(x, y, z)\,dxdy. \tag{22}$$

Again, we prefer to write this as duality pairing between a 2-form and a two-dimensional surface,

$$\langle \eta^{(2)}, \mathcal{S} \rangle := \int_{\mathcal{S}} \eta^{(2)}. \tag{23}$$

This duality form is not just snobbery, it will later allow us to identify the vector operations **grad**, **curl**, and **div** as the formal adjoints of the boundary operator. A similar identification will immediately give us the discrete analogues of these vector operations at the discrete level.

The basis vectors for the 2-form are given by $dydz$, $dzdx$, and $dxdy$. Note that combinations like $dxdx$ and $dydx$ are missing from this expansion. This is due to the fact that, for instance, $dxdy$ is an abbreviated form of the so-called *wedge product*: $dx \wedge dy$ and this wedge product is anti-symmetric, i.e.,

$$dx \wedge dy = -dy \wedge dx. \tag{24}$$

This shows that $dx \wedge dx = dy \wedge dy = dz \wedge dz \equiv 0$. We will come back to the wedge product in the next section. Let us first introduce the last two types of differential forms in $\mathbb{R}^3$: the 0-form and the 3-form. A 3-form is given by

$$\omega^{(3)} = g(x, y, z)\,dxdydz. \tag{25}$$

The 3-forms are associated with integration over volumes

$$\int_{\mathcal{V}} \omega^{(3)} = \int_{\mathcal{V}} g(x, y, z)\, dxdydz. \tag{26}$$

And again we associate this with duality pairing between the 3-form and three-dimensional objects

$$\left\langle \omega^{(3)}, \mathcal{V} \right\rangle = \int_{\mathcal{V}} \omega^{(3)}. \tag{27}$$

A 0-form is given by

$$\alpha^{(0)} = f(x, y, z). \tag{28}$$

This is just a scalar function defined at certain points in the domain. In order to extend our definitions to integration over a collection of points, say $\mathcal{P}_1, \ldots, \mathcal{P}_k$, we define the integral of 0-forms as

$$\int_{\mathcal{P}_1,\ldots,\mathcal{P}_k} \alpha^{(0)} = \sum_{i=1}^{k} f(\mathcal{P}_i), \tag{29}$$

and analogous to the previous cases we define the duality pairing as

$$\left\langle \alpha^{(0)}, \mathcal{P} \right\rangle = f(\mathcal{P}). \tag{30}$$

Here again we see that both the 0-form and the 3-form are described by scalar fields, f and g, respectively, but there is a different association with respect to geometry.

3.2. The Wedge Product

The wedge product is a product between k-forms and l-forms and it produces a $(k+l)$-form. Let the space of k-forms in Ω be denoted by $\Lambda^k(\Omega)$ and the space of l-forms be given by $\Lambda^l(\Omega)$, then

$$\wedge \;:\; \Lambda^k(\Omega) \times \Lambda^l(\Omega) \;\longrightarrow\; \Lambda^{k+l}(\Omega). \tag{31}$$

The wedge product is multi-linear, so if $a, b \in \Lambda^k(\Omega)$ and $c, d \in \Lambda^l(\Omega)$ then

$$\begin{aligned}(\alpha a + \beta b) \wedge (\gamma c + \delta d) = \alpha\gamma\,(a \wedge c) + \alpha\delta\,(a \wedge d) \\ + \beta\delta\,(b \wedge d) + \beta\delta(b \wedge c),\end{aligned} \tag{32}$$

for $\alpha,\ \beta,\ \gamma,\ \delta \in \mathbb{R}$. The wedge product is associative

$$(a \wedge b) \wedge c = a \wedge (b \wedge c) = a \wedge b \wedge c. \tag{33}$$

For general k-forms, a, and l-forms, b, we have

$$a \wedge b = (-1)^{kl}\, b \wedge a, \tag{34}$$

and, therefore, we have that for any odd k-form a

$$a \wedge a \equiv 0. \tag{35}$$

For instance this implies that $dx \wedge dx \equiv 0$ as was mentioned in the previous section. Furthermore, this implies that

$$\begin{aligned}0 = (dx + dy) \wedge (dx + dy) = dx \wedge dx + dx \wedge dy \\ + dy \wedge dx + dy \wedge dy = dx \wedge dy + dy \wedge dx.\end{aligned} \tag{36}$$

So this implies the anti-symmetry mentioned before

$$dx \wedge dy = -dy \wedge dx. \tag{37}$$

These properties of the wedge product will be used in the remainder of this article.

3.3. Transformations

In computational mechanics, it is generally useful to use mappings between a reference domain and the actual physical domain. Such transformations are either convenient, such as in finite element methods, where computations in a finite element are usually performed in a reference element, or part of the description of the kinematics [28, Chapter 1]. Let us, therefore, briefly look how differential forms behave under transformations. In fact, this section can be kept short, since we already know how integrals behave under transformations and the differential forms are closely connected to integration theory.

Suppose we are given a change of variables

$$\begin{cases} u = u(x, y, v) \\ v = v(x, y, z) \\ w = w(x, y, z) \end{cases} \iff \begin{cases} x = x(u, v, w) \\ y = y(u, v, w) \\ z = z(u, v, w) \end{cases}. \tag{38}$$

Then the 1-form $\lambda^{(1)} = A dx + B dy + C dz$ transforms like

$$\begin{aligned}\lambda^{(1)} &= A(x, y, z)\, dx + B(x, y, z)\, dy + C(x, y, z)\, dz \\ &= A(u, v, w)\left[\frac{\partial x}{\partial u}\, du + \frac{\partial x}{\partial v}\, dv + \frac{\partial x}{\partial w}\, dw\right] \\ &\quad + B(u, v, w)\left[\frac{\partial y}{\partial u}\, du + \frac{\partial y}{\partial v}\, dv + \frac{\partial y}{\partial w}\, dw\right] \\ &\quad + C(u, v, w)\left[\frac{\partial z}{\partial u}\, du + \frac{\partial z}{\partial v}\, dv + \frac{\partial z}{\partial w}\, dw\right] \\ &= \left(A\frac{\partial x}{\partial u} + B\frac{\partial y}{\partial u} + C\frac{\partial z}{\partial u}\right) du \\ &\quad + \left(A\frac{\partial x}{\partial v} + B\frac{\partial y}{\partial v} + C\frac{\partial z}{\partial v}\right) dv \\ &\quad + \left(A\frac{\partial x}{\partial w} + B\frac{\partial y}{\partial w} + C\frac{\partial z}{\partial w}\right) dw.\end{aligned} \tag{39}$$

So (39) tells us how the vector proxies transform when under the mapping $(x, y, z) \to (u, v, w)$. Another way to write the

1-form in (u, v, w)-coordinates is to use a change of variables for integrals. Following the same steps and using the fact that the wedge product is anti-symmetric, we can show that a 2-form transforms as

$$\begin{aligned}\eta^{(2)} &= P(x,y,z)\,dydz + Q(x,y,z)\,dzdx + R(x,y,z)\,dxdy \\ &= \left[P\left(\frac{\partial y}{\partial v}\frac{\partial z}{\partial w} - \frac{\partial y}{\partial w}\frac{\partial z}{\partial v}\right) + Q\left(\frac{\partial z}{\partial v}\frac{\partial x}{\partial w} - \frac{\partial z}{\partial w}\frac{\partial x}{\partial v}\right)\right. \\ &\quad \left. + R\left(\frac{\partial x}{\partial v}\frac{\partial y}{\partial w} - \frac{\partial x}{\partial w}\frac{\partial y}{\partial v}\right)\right] dvdw \\ &\quad + \left[P\left(\frac{\partial y}{\partial w}\frac{\partial z}{\partial u} - \frac{\partial y}{\partial u}\frac{\partial z}{\partial w}\right) + Q\left(\frac{\partial z}{\partial w}\frac{\partial x}{\partial u} - \frac{\partial z}{\partial u}\frac{\partial x}{\partial w}\right)\right. \\ &\quad \left. + R\left(\frac{\partial x}{\partial w}\frac{\partial y}{\partial u} - \frac{\partial x}{\partial u}\frac{\partial y}{\partial w}\right)\right] dwdu \\ &\quad + \left[P\left(\frac{\partial y}{\partial u}\frac{\partial z}{\partial v} - \frac{\partial y}{\partial v}\frac{\partial z}{\partial u}\right) + Q\left(\frac{\partial z}{\partial u}\frac{\partial x}{\partial w} - \frac{\partial z}{\partial v}\frac{\partial x}{\partial u}\right)\right. \\ &\quad \left. + R\left(\frac{\partial x}{\partial u}\frac{\partial y}{\partial v} - \frac{\partial x}{\partial v}\frac{\partial y}{\partial u}\right)\right] dudv. \end{aligned} \tag{40}$$

So the vector proxies associated with 2-forms transform according to (40). This is different from the transformation of 1-forms. In vector calculus, both quantities are described by vectors and the difference only shows up in coordinate transformations. I leave it as a simple exercise to determine how 0-forms and 3-forms transform.

Another way to write the transformations of k-forms is by using the so-called *pullback operator*. Suppose the mapping is defined by $\Phi : (x, y, z) \to (u, v, w)$ and we have a differential form, $a^{(k)}$ given in (u, v, w) coordinates, then we have

$$\begin{aligned}\int_{\Phi(\mathcal{M}^k)} a^{(k)} &= \int_{\mathcal{M}^k} \Phi^* a^{(k)} \iff \langle \Phi(\mathcal{M}^k), a^{(k)} \rangle \\ &= \langle \mathcal{M}^k, \Phi^* a^{(k)} \rangle. \end{aligned} \tag{41}$$

So if Φ maps the geometry from $(x, y, z) \to (u, v, w)$, the pullback operator, Φ^*, takes k-forms defined in (u, v, w) to the k-form in (x, y, z). This explains its suggestive name. Here $\mathcal{M}^k$ is a regular k-dimensional manifold such as the points, curves, surfaces and volumes discussed previously and $a^{(k)}$ a differentiable k-form defined on the manifold $\mathcal{N}^k$ obtained by the mapping $\Phi : \mathcal{M}^k \longrightarrow \mathcal{N}^k$. This is just a change of variables in integration theory.

The importance of the pullback operator is that it commutes with the wedge product, i.e., for every k-form, $a^{(k)}$, and l-form, $b^{(l)}$, we have

$$\left(\phi^* a^{(k)}\right) \wedge \left(\phi^* b^{(l)}\right) = \phi^* \left(a^{(k)} \wedge b^{(l)}\right), \tag{42}$$

showing that the wedge product is a canonical coordinate free operation. Furthermore, it also commutes with the exterior derivative that will be discussed in the next section. So we also have that for every $a^{(k)}$

$$\phi^* \left(da^{(k)}\right) = d\left(\phi^* a^{(k)}\right). \tag{43}$$

The exterior derivative is, therefore, also coordinate free.

3.4. The Exterior Derivative

The exterior derivative, d, is an operation on k-forms, which transforms k-forms in $(k+1)$-forms and if one applies the exterior derivative twice it transforms a k-form into $0^{(k+2)}$, i.e., the zero $(k+2)$-form: $d \circ d\beta^{(k)} = 0^{(k+2)}$. Let us see in practice how this operator acts on the various differential forms.

3.4.1. Exterior Derivative of 0-Form

Let the 0-form $\alpha^{(0)}$ be given by $\alpha^{(0)} = f(x, y, z)$, then the exterior derivative $d\alpha^{(0)}$ is given by

$$d\alpha^{(0)} = \frac{\partial f}{\partial x}\,dx + \frac{\partial f}{\partial y}\,dy + \frac{\partial f}{\partial z}\,dz. \tag{44}$$

So if we associate the vector proxy of the 0-form with $f(x, y, z)$, then the vector proxy of $d\alpha^{(0)}$ is **grad** f.

3.4.2. Exterior Derivative of 1-Form

Let the 1-form $\lambda^{(1)}$ be given by $\lambda^{(1)} = A\,dx + B\,dy + C\,dz$ then its exterior derivative is given by

$$\begin{aligned} d\lambda^{(1)} &= \left(\frac{\partial A}{\partial x}\,dx + \frac{\partial A}{\partial y}\,dy + \frac{\partial A}{\partial z}\,dz\right) \wedge dx + Ad \circ dx \\ &\quad + \left(\frac{\partial B}{\partial x}\,dx + \frac{\partial B}{\partial y}\,dy + \frac{\partial B}{\partial z}\,dz\right) \wedge dy + Bd \circ dy \\ &\quad + \left(\frac{\partial C}{\partial x}\,dx + \frac{\partial C}{\partial y}\,dy + \frac{\partial C}{\partial z}\,dz\right) \wedge dz + Cd \circ dz \\ &= \left(\frac{\partial C}{\partial y} - \frac{\partial B}{\partial z}\right) dydz + \left(\frac{\partial A}{\partial z} - \frac{\partial C}{\partial x}\right) dzdx \\ &\quad + \left(\frac{\partial B}{\partial x} - \frac{\partial A}{\partial y}\right) dxdy. \end{aligned} \tag{45}$$

So if $\mathbf{u} = (A, B, C)$ is the vector proxy of the 1-form, then the vector proxy of $d\lambda^{(1)}$ is given by **curl u**.

3.4.3. Exterior Derivative of 2-Form

Let the 2-form $\eta^{(2)}$ be given by $\eta^{(2)} = P\,dydz + Q\,dzdx + R\,dxdy$ then it is easy to establish that its exterior derivative is given by

$$d\eta^{(2)} = \left(\frac{\partial P}{\partial x} + \frac{\partial Q}{\partial y} + \frac{\partial R}{\partial z}\right) dxdydx. \tag{46}$$

So if $\mathbf{v} = (P, Q, R)$ is the vector proxy of $\eta^{(2)}$, the **div v** is the vector proxy of $d\eta^{(2)}$. Since we are working in $\mathbb{R}^3$ it is easy to show that the exterior derivative of a 3-form vanishes identically.

So the exterior derivative, d, plays the role of the vector operators discussed in section 2. Furthermore, the fact that $d \circ d \equiv 0$, gives in $\mathbb{R}^3$, in terms of the vector proxies the identities

$$\mathbf{curl} \cdot \mathbf{grad} \equiv 0 \quad \text{and} \quad \mathbf{div} \cdot \mathbf{curl} \equiv 0. \tag{47}$$

Let $\Lambda^k(\Omega)$ be the set of k-forms defined on Ω, then we can rewrite the De Rham sequence, (17), in terms of differential forms

$$\mathbb{R} \hookrightarrow \Lambda^0(\Omega) \xrightarrow{d} \Lambda^1(\Omega) \xrightarrow{d} \Lambda^2(\Omega) \xrightarrow{d} \Lambda^3(\Omega) \xrightarrow{d} 0. \tag{48}$$

So from now on we replace the suggestive names H_P, H_L, H_S, and H_V by Λ^k, $k = 0, 1, 2, 3$.

One of the important properties of the exterior derivative is that it commutes with the pullback operator. So if ϕ is a coordinate transformation from a reference domain to physical space, then ϕ^* maps differential forms in physical space to differential forms on the reference domain. The commutation property implies that we can take derivatives in physical space and transform to the reference domain, or first transform the physical quantity to the reference domain and then take the derivative. This property will be exploited on distorted grids, see Example 4. in section 5.

3.5. The Generalized Stokes Theorem

In the previous section, we saw that the vector operations **grad**, **curl**, and **div** are representations of the exterior derivative depending on the space Λ^k. In section 2, we also encountered the integral theorems these vector operators satisfy. Now these integral theorems can also be cast in a single format in terms of differential geometry and this theorem is called the *generalized Stokes Theorem*. Let $\eta^{(k)} \in \Lambda^k$ and $\mathcal{C}_{k+1}$ be a regular, $(k+1)$-dimensional manifold with boundary $\partial\mathcal{C}_{k+1}$ then we have

$$\int_{\mathcal{C}} d\eta^{(k)} = \int_{\partial\mathcal{C}} \eta^{(k)}. \tag{49}$$

For $k = 0$ this equation gives the gradient integral theorem, for $k = 1$ this yields the classical Stokes theorem and for $k = 2$ we have the divergence theorem. Recall that we also interpreted integration as duality pairing between differential forms and k-dimensional manifolds. In this form, the generalized Stokes Theorem is given by

$$\left\langle d\eta^{(k-1)}, \mathcal{C}_k \right\rangle = \left\langle \eta^{(k-1)}, \partial\mathcal{C}_k \right\rangle. \tag{50}$$

This relation reveals that the exterior derivative, d, is in fact the formal adjoint of the boundary operator ∂. This means that the exterior derivative can be defined without any assumptions on differentiability or smoothness. This is important in computational methods, where solutions are generally not globally smooth and differentiable, but the geometric elements in the grid (points, curves, surfaces, and volumes) and their respective boundaries are generally well defined.

Many of the concepts introduced in this section have a natural discrete counterpart in algebraic topology, which we will study in the next section. Unfortunately, not all concepts can be represented on a discrete level. One of the operators that has no discrete analogue is the Hodge-$\star$ operator that we will study next.

3.6. The Hodge-$\star$ Operator

The appearance of the Hodge-$\star$ operator is best illustrated by an example. Consider the Poisson equation $\Delta\phi = f$ as a first order system:

$$\mathbf{div}\, \mathbf{q} = f, \tag{51}$$

$$\mathbf{grad}\, \phi = \mathbf{u}, \tag{52}$$

and

$$\mathbf{u} = \mathbf{q}. \tag{53}$$

It may be surprising to learn that the equations (52) and (52) are the easiest ones to discretize. In fact, these two relations can be approximated exactly in the discrete sense. It is the apparently innocent looking Eq. (53) where all approximations take place.

Now from the preceding sections, we see that **div** acts on 2-forms, so we will interpret **q** as the vector proxy of the 2-form $q^{(2)}$. Then f must be a vector proxy of the 3-form $f^{(3)}$, so we can rewrite (52) in differential form as

$$dq^{(2)} = f^{(3)}. \tag{54}$$

Let us now consider the second equation, (52), and convert this to differential form. We know that **grad** is the vector proxy of the exterior derivative of a 0-form, so let ϕ be the vector proxy of the 0-form $\phi^{(0)}$. Since the exterior derivative maps 0-forms onto 1-forms, **u** on the right-hand side of (52) must be a 1-form. So (52) in differential form reads

$$d\phi^{(0)} = u^{(1)}. \tag{55}$$

The last equation of the Poisson equation, (53), then would read: $u^{(1)} = q^{(2)}$, which is clearly not possible. This is again a situation where vector calculus obscures the difference between two types of vectors and where the difference in terms of differential geometry is apparent.

However, there is a linear operator, the Hodge-$\star$ operator, which maps k-forms onto $(n-k)$-forms, where n is the dimension of the ambient space. This operator is based on the inner-product and is defined as: Let $\eta^{(k)}$ a k-form and let $\lambda^{(n-k)}$ be any $(n-k)$-form with vector proxy λ, then the vector proxy

$\star\eta$ is defined by

$$(\star\eta, \lambda)\,\omega^{(n)} = \eta^{(k)} \wedge \lambda^{(n-k)}, \quad \forall\lambda^{(n-k)} \in \Lambda^{(n-k)}, \tag{56}$$

where $\omega^{(n)}$ is the volume element $\omega^{(n)} = dxdydz$. Then $\star\eta$ is the vector proxy of the $(n-k)$-form $\star\eta^{(k)}$. In layman's terms, the Hodge operator does not alter the scalar field or the vector field, but changes the geometric object with which these fields are associated. Consider for example, the 1-form

$$\begin{aligned} a^{(1)} &= a_1(x, y, z)\,dx + a_2(x, y, z)\,dy + a_3(x, y, z)\,dz \\ &\Longrightarrow \\ \star a^{(1)} &= a_1(x, y, z)\,dydz + a_2(x, y, z)\,dzdx \\ &\quad + a_3(x, y, z)\,dxdy. \end{aligned}$$

Application of the Hodge-$\star$ operator twice gives plus or minus the identity

$$\star\star\, a^{(k)} = (-1)^{k(n-k)} a^{(k)}. \tag{57}$$

Now that we have a mapping from k-forms to $(n-k)$-forms, we can set up a second De Rham complex in reversed order and connect the two complexes by the $\star$-operator as shown in (58):

$$\begin{array}{ccccccccccccc} \mathbb{R} & \longrightarrow & \Lambda^0(\Omega) & \xrightarrow{d} & \Lambda^1(\Omega) & \xrightarrow{d} & \Lambda^2(\Omega) & \xrightarrow{d} & \Lambda^3(\Omega) & \xrightarrow{d} & 0 \\ & & \updownarrow\star & & \updownarrow\star & & \updownarrow\star & & \updownarrow\star & & \\ 0 & \xleftarrow{d} & \Lambda^3(\Omega) & \xleftarrow{d} & \Lambda^2(\Omega) & \xleftarrow{d} & \Lambda^1(\Omega) & \xleftarrow{d} & \Lambda^0(\Omega) & \longleftarrow & \mathbb{R} \end{array} \tag{58}$$

In fact, the $\star$-operator is more than just a nice mathematical trick to resolve our problem with the Poisson equation in differential form. The theory behind this operator is based on the two types of orientation every geometric object possesses: inner orientation (independent of the dimension of the ambient space in which this geometric object is embedded) and outer orientation (which depends on the dimension and orientation of the ambient space). It is beyond the scope of this article to spend more time on these two types of orientation, but I recommend you to consult Mattiussi [2] and Bossavit's Japanese papers [3], for more information. Understanding of the geometric nature of physical variables and the connection between different types of orientation is well worth the effort if one wants to fully understand mimetic methods. Tonti [1] classifies both branches in (58) in terms of a different physical nature. One De Rham complex is associated with *configuration variables*, while the dual De Rham complex is associated with the *source variables*. The Hodge-$\star$ operator connects configuration variables with the source variables. Such connections are known in physics and engineering as *constitutive equations* or *rheological equations of state*. Tonti demonstrates that relations between configuration variables can be represented discretely in a metric-free way without error. The same holds for relations among source variables. But modeling of the constitutive equations requires metric and needs to be done with a continuous description. So any model that does not contain a constitutive model can be represented in a metric-free way and a compatible scheme will always give an exact solution, no matter how coarse or ill-deformed the grid is. We will show examples of this fact in section 5.

The (numerical) approximation takes place when we discretize the Hodge-$\star$ operator. The numerical error in our simple Poisson problem is thus generated by this approximation only and *not* by the discretization of the divergence or gradient relation which can be discretized exactly. According to Perot this is the most suitable place to make approximations, because constitutive models form the mathematical approximation/model of how we think a material behaves. If this is the place where we make physical assumptions/approximations, then it also seems the most suitable place to make our numerical approximations.

Using the Hodge-$\star$ operator we can write the last equation in terms of differential geometry as

$$q^{(2)} = \star u^{(1)}. \tag{59}$$

This more or less completes the description of a very simple model problem in terms of differential geometry. In the next section, we will encounter many of the concepts discussed so far, but now in a discrete, metric-free setting. However, the Hodge-$\star$ has no discrete counterpart and we have to wait until section 5 before we can tackle that problem.

With the differential forms introduced in this section, we can now write conservation of mass, introduced in section 2, as

$$d\rho^{(3)} + d\,(\rho u)^{(3)} = 0, \tag{60}$$

with

$$\rho^{(3)} = \rho(x, y, z, t)\,dxdydz, \tag{61}$$

and

$$\begin{aligned} (\rho u)^{(3)} &= \rho u(x, y, z, t)\,dydzdt + \rho v(x, y, z, t)\,dzdtdx \\ &\quad + \rho w(x, y, z, t)\,dtdxdy. \end{aligned} \tag{62}$$

4. ALGEBRAIC TOPOLOGY

As was alluded to several times before, there is a discrete analogue of the aforementioned differential geometry, which is worth studying in itself. It is surprising how many mathematical concepts used in engineering have a purely topological basis and can be defined without concepts, such as metric, norm, angle, inner-product, etc. For the sake of computation, it is worth remembering that all topological concepts can be expressed

exactly, independent of the grid. It is the metric part, which is not captured by algebraic topology, that requires approximations and, therefore, depends on the quality of the grid. It turns out that we can separate these two parts—the metric-free, topological part and the metric part. This will be demonstrated in section 5 where we apply these ideas to spectral element formulations.

The first thing we need is a topological description of the geometry.[1] Therefore, we need the concept of p-cells. 0-cells are points or zero-dimensional objects in topological space. We cannot tell where these points are or what the distance between these points is, because in topology distance and an origin with respect to which we can determine the location does not exist. If we have finitely many of such 0-cells, $c_{(0),i}$, labeled by P_i, $i = 1, \ldots, n_P$ we can form the formal sum

$$C_0 = \sum_{i=1}^{n_P} m_{(0),i} c_{(0),i}, \tag{63}$$

called a 0-chain. The weights $m_{(0),i}$ in the 0-chain can be taken from $\mathbb{R}$ (or any field $\mathcal{F}$), but for our purpose it suffices to allow only the values $m_{(0),i} = 1$, which means that the 0-cell $c_{(0),i}$ is part of the chain and its orientation is unaltered. The value $m_{(0),i} = -1$ means that the 0-cell, $c_{(0),i}$ is part of the chain, but its orientation is reversed and finally $m_{(0),i} = 0$ means that $c_{(0),i}$ is not part of the 0-chain. Mattiussi [2] interprets chains with weights in $\mathbb{R}$ in terms of finite element methods. Let us set the default orientation of 0-cells to be positive.

Let us connect a number of 0-cells with line segments (not neccesarily bounded by 0-cells). These line segments are called 1-cells, $c_{(1)}$. It is not clear whether these lines are straight, curved, self-intersecting, because in topological space only the relation between the various objects is of importance. Label all the 1-cells by L_i, $i = 1, \ldots, n_L$. You are completely free to label the 1-cells any way you like. Also, choose an orientation for all the 1-cells. Suppose that the 1-cell labeled L_k connects the two 0-cells P_q and P_r then either choose the direction from P_q to P_r positive or the direction P_r to P_q. What you choose is not important as long as you make a choice and stick to this orientation for the rest of the analysis. Just like the 0-chain, we can now formally define the sum

$$C_1 = \sum_{i=1}^{n_L} m_{(1),i} c_{(1),i}, \tag{64}$$

called a 1-chain. Again we restrain the values of $m_{(1),i}$ to be 1 (orientation unaltered), -1 (orientation reversed), and 0 (1-cell not in the chain).

[1]In this section, we will work with cubical complexes consisting of singular n-cubes [27, 29] and not simplicial complexes [30, 31]. There is, however, a natural isomorphism from the singular homology to the cubical homology [32].

A 2-cell is a surface bounded by 1-cells. Again the actual shape of the surface is irrelevant. Let us endow this surface with an inner orientation by looking at the surface and by imposing a positive orientation in the clockwise or counter-clockwise direction. The actual choice of which side of the surface you look at and whether you decide whether clockwise or counter-clockwise is positive is again irrelevant. All you need is an oriented two-dimensional object and stick to your choice from then on. After labeling all the 2-cells by S_i, $i = 1, \ldots, n_S$, the formal sum is given by

$$C_2 = \sum_{i=1}^{n_S} m_{(2),i} c_{(2),i}, \tag{65}$$

called a 2-chain. The values allowed for $m_{(2),i}$ and their meaning should be clear by now.

In a similar way, we can define p-cells and the p-chain as the formal sum for $p > 2$. If we treat time as a separate dimension the case $p = 4$ is appropriate for time dependent problems in 3D. The collection of all the p-cells is called the *cell complex*. A small two-dimensional, oriented cell-complex is given in Figure 1.

With the labeling and the orientation established for a given cell-complex, we can determine the boundary of the various p-cells. The boundary of 0-cells is empty, i.e., points have no boundary. The boundary of 1-cell, labeled L_2 in Figure 1, is given by the 0-chain $P_3 - P_2$ and the boundary for the 1-cell labeled L_3 is given by the 0-chain $P_3 - P_4$. So for the simple

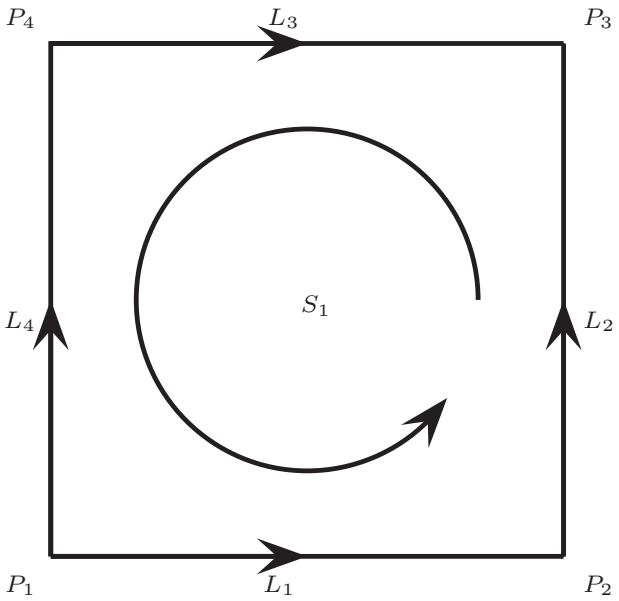

FIG. 1. Two-dimensional, oriented cell-complex.

sample complex in Figure 1 we have

$$\partial \begin{pmatrix} L_1 \\ L_2 \\ L_3 \\ L_4 \end{pmatrix} = \begin{pmatrix} \partial L_1 \\ \partial L_2 \\ \partial L_3 \\ \partial L_4 \end{pmatrix} = \begin{pmatrix} -1 & 1 & 0 & 0 \\ 0 & -1 & 1 & 0 \\ 0 & 0 & 1 & -1 \\ -1 & 0 & 0 & 1 \end{pmatrix} \begin{pmatrix} P_1 \\ P_2 \\ P_3 \\ P_4 \end{pmatrix}, \tag{66}$$

where ∂ denotes the boundary operator. Equation (66) shows that the boundary operator acting on the 1-cells can be represented by a matrix consisting of only the values -1, 1, and 0. This matrix is called the *incidence matrix* and will be denoted by $\mathbb{E}^{1,0}$, where the superscript indicates that it relates the boundary of 1-cells to the 0-cells.

In a similar way, we can determine the boundary of the surface S_1, which is given by $L_1 + L_2 - L_3 - L_4$. The signs in this boundary 1-chain are determined as follows: If you move in the positive direction in the surface close to the boundary, either the orientation of the bounding 1-cell agrees which gives a $+$-sign or is opposite, yielding a $-$sign. The incidence matrix $\mathbb{E}^{2,1}$ is, thus, given by

$$\begin{aligned} \partial S_1 \;&=\; \mathbb{E}^{2,1} L_i = \begin{pmatrix} 1 & 1 & -1 & -1 \end{pmatrix} \begin{pmatrix} L_1 \\ L_2 \\ L_3 \\ L_4 \end{pmatrix} \\ \Longrightarrow \quad & \mathbb{E}^{2,1} = \begin{pmatrix} 1 & 1 & -1 & -1 \end{pmatrix} \end{aligned} \tag{67}$$

Figure 1 only shows a very small cell-complex, but if more points, line segments, and surfaces are included, such a cell-complex resembles a mesh used in many computational methods. I reiterate that, although a nice orthogonal complex is depicted in Figure 1, the precise shape is irrelevant because it is only the connectivity that matters. The boundary operator is a very important ingredient in computational methods. As we have seen in section 3.1., Eq. (50), the exterior derivative is defined as the formal adjoint of the boundary operator through the generalized Stokes Theorem. Once we have defined variables acting on the p-cells, we can define a discrete exterior derivative along the same lines. So let us define the p-cochain.

A p-cochain is a list of numbers, $a_i^{(p)}$, $i = 1, \ldots, n_p$ where each number $a_i^{(p)} \in \mathbb{R}$ is associated with the p-cell. A p-cochain can also be written as a formal sum like

$$C^{(p)} = \sum_{i=1}^{n_p} a_i^{(p)} c_i^{(p)}. \tag{68}$$

If we apply this p-cochain to a p-chain by means of duality pairing we get

$$\left\langle C^{(p)}, C_{(p)} \right\rangle = \sum_{i=}^{n_p} \sum_{j=1}^{n_p} a_i^{(p)} m_{(p),j} \left\langle c_i^{(p)}, c_{(p),j} \right\rangle. \tag{69}$$

Now $\left\langle c_i^{(p)}, c_{(p),j} \right\rangle = \delta_{ij}$, so this yields

$$\left\langle C^{(p)}, C_{(p)} \right\rangle = \sum_{i=}^{n_p} a_i^{(p)} m_{(p),j}. \tag{70}$$

This expression resembles the integration of a p-form over a p-dimensional manifold, where the cochain plays the role of the differential form and the chain plays the role of the manifold. For $p = 0$, this expression should be compared with (30), for $p = 1$ with (20), for $p = 2$ with (23), and for $p = 3$ with (27).

Now we are in a position to define the *coboundary operator*, δ. For all $(p+1)$-chains and p-cochains, define the coboundary operator as

$$\left\langle \delta C^{(p)}, C_{(p+1)} \right\rangle := \left\langle C^{(p)}, \partial C_{(p+1)} \right\rangle. \tag{71}$$

The coboundary operator maps p-cochains onto $(p+1)$-cochains, just like the exterior derivative maps k-forms onto $(k+1)$-forms. The coboundary operator is the formal adjoint of the boundary operator, just like the exterior derivative is the formal adjoint of the boundary operator in the continuous case due to the generalized Stokes Theorem, see (50). Moreover, we have that $\delta \circ \delta \equiv 0$. This is due to the fact that the boundary of the boundary of any p-chain is zero, see [27, 30], which is illustrated in Figure 2. This implies that

$$\begin{aligned} \left\langle \delta \circ \delta C^{(p)}, C_{(p+2)} \right\rangle = \left\langle \delta C^{(p)}, \partial C_{(p+2)} \right\rangle &= \left\langle C^{(p)}, \partial \circ \partial C_{(p+2)} \right\rangle \\ &= \left\langle C^{(p)}, 0 \right\rangle = 0. \end{aligned} \tag{72}$$

These properties of the coboundary operator allow us to set up a De Rham complex for p-cochains

$$0 \hookrightarrow C^{(0)} \xrightarrow{\delta} C^{(1)} \xrightarrow{\delta} C^{(2)} \xrightarrow{\delta} C^{(3)} \xrightarrow{\delta} 0. \tag{73}$$

By analogy to the exterior derivative, the coboundary applied to 0-cochains will play the role as discrete gradient, the coboundary operator applied to 1-cochains will play the role as the discrete curl operator and the coboundary operator applied to 2-cochains will act as our discrete divergence operator. Note that all these discrete vector operators are metric-free and independent of the precise shape of the geometry (= cell-complex). Furthermore, since we have a matrix representation for the boundary operator, the incidence matrices $\mathbb{E}^{p+1,p}$, we also a have a matrix representation for our discrete vector operators. The property that $\delta \circ \delta \equiv 0$ can now be interpreted in terms of our discrete vector operators as the discrete curl applied to the discrete gradient vanishes and the discrete divergence applied to the discrete curl vanishes also.

Before we move on to an implementation in terms of spectral elements, let us look how we can incorporate the second De Rham complex—i.e., the bottom row in (58)—into our algebraic

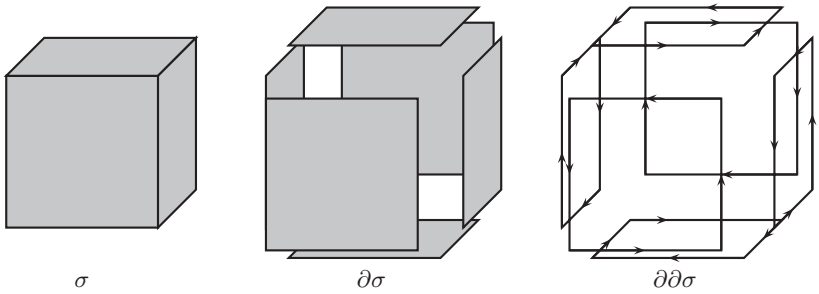

FIG. 2. $\partial \circ \partial \equiv 0$.

topological framework. We need this second De Rham complex to associate k-forms with $(n-k)$-forms. This can be established by associating with each p-cell in our primal grid a $(n-p)$-cell.

In Figure 3, our initial simple cell complex (Figure 1) is shown in light gray and the dual complex is inserted in black. One sees that with each 0-cell in the primal complex there is now a 2-cell in dual complex. With all 1-cells in the primal complex, we now associate 1-cells in the dual complex and, finally, with the 2-cell in the primal complex we associate a 0-cell in the dual complex. The labeling of the $(n-p)$-cells conforms to the labeling of the associated p-cells on the primal complex: If a 0-cell on the primal complex is label P_i, then the dual 2-cell is label $\tilde{S}_i$ on the dual complex, where the twiddle indicates that this 2-cell is in the dual complex.

In the same way as we did for the primal complex, we can now associate values to the dual p-cells, the *dual p-cochain*. Using the boundary operator in the dual complex, we can set up the coboundary operator for dual cochains. Because we can represent the boundary operator by the incidence matrices, we also have a matrix representation for the coboundary operators on the dual complex. Let us denote the incidence matrices on the dual complex by $\mathbb{F}^{p+1,p}$, then we have from Figure 3 that

$$\mathbb{F}^{1,0} = \begin{pmatrix} 1 \\ 1 \\ -1 \\ -1 \end{pmatrix} \quad \text{and} \quad \mathbb{F}^{2,1} = \begin{pmatrix} 1 & 1 & 0 & 0 \\ -1 & 1 & 0 & 0 \\ 0 & -1 & -1 & 0 \\ 0 & 0 & 1 & -1 \end{pmatrix}. \tag{74}$$

Note that $\mathbb{F}^{1,0} = (\mathbb{E}^{2,1})^T$ and $\mathbb{F}^{2,1} = (\mathbb{E}^{1,0})^T$ (or on n-dimensional cell-complexes $\mathbb{F}^{p+1,p} = (\mathbb{E}^{n-p,n-p-1})^T$). This property also holds for the adjoint matrices and, therefore, we have that the *discrete divergence operator on the dual complex* is the transpose of *discrete gradient operator on the primal complex*. These adjointness relations also hold between the curl on the primal and curl on the dual complex and the gradient on the primal and the divergence on the dual complex. This is one of the properties that ensures that the discrete Laplace operator will be symmetric, irrespective of the shape of the grid, since all ingredients used so far are purely topological.

These ingredients allow us to represent the extended De Rham complex on the two dual meshes by

$$\begin{array}{ccccccccccc} \mathbb{R} & \longrightarrow & C^0(K) & \xrightarrow{\delta} & C^1(K) & \xrightarrow{\delta} & C^2(K) & \xrightarrow{\delta} & 0 \\ & & \updownarrow{\scriptstyle \star^h} & & \updownarrow{\scriptstyle \star^h} & & \updownarrow{\scriptstyle \star^h} & & \\ 0 & \xleftarrow{\delta} & \tilde{C}^2(\tilde{K}) & \xleftarrow{\delta} & \tilde{C}^1(\tilde{K}) & \xleftarrow{\delta} & \tilde{C}^0(\tilde{K}) & \longleftarrow & \mathbb{R}, \end{array} \tag{75}$$

where $C^p(K)$ denotes the space of p-cochains on the primal cell-complex K and $\tilde{C}^p(\tilde{K})$ the space of cochains on the dual cell-complex $\tilde{K}$. Note that the operator that connects the dual cochains is the discrete Hodge-$\star$ operator, $\star^h$, which cannot be described in terms of algebraic topology.

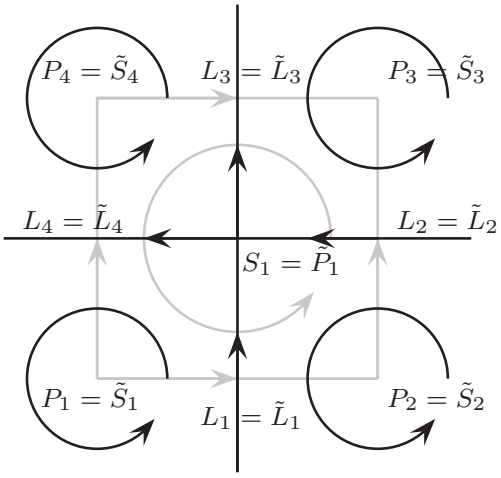

FIG. 3. Dual cell complex.

5. SPECTRAL IMPLEMENTATION

In the previous sections, it was shown that familiar operations in vector calculus can be adequately represented by differential geometry and that the basic vector operators (**grad**, **curl**, and **div**) can also be represented in a completely metric-free, topological setting as the formal adjoint of the boundary operator.

In this section, we want to establish a connection between differential forms and cochains. What we need is an operation that converts differential forms into cochains, which we will call *reduction* and an operation that converts cochains into differential forms, which we will call *reconstruction*, see [13].

5.1. The Reduction Operator

Let the domain of interest, an n-dimensional manifold Ω, be covered by a cell-complex, such that all p-chains are p-dimensional submanifolds of Ω. Let $a^{(p)} \in \Lambda^p(\Omega)$ be a differential form. Then the reduction operation is defined as

$$\langle \mathcal{R}a^{(p)}, C_{(p)} \rangle := \int_{C_{(p)}} a^{(p)}, \tag{76}$$

in which $\mathcal{R}a^{(p)}$ is a p-cochain acting on a p-chain, $C_{(p)}$. Therefore, the reduction operator $\mathcal{R}$ maps a p-form onto a p-cochain. Using the linearity of the duality pairing on chains we have

$$\begin{aligned} \left\langle \mathcal{R}a^{(p)}, C_{(p)} = \left\langle \mathcal{R}a^{(p)}, \sum_{i=1}^{n_p} m_{(p),i} c_{(p),i} \right\rangle \right. \\ = \sum_{i=1}^{n_p} m_{(p),i} \left\langle \mathcal{R}a^{(p)}, c_{(p),i} \right\rangle. \end{aligned}$$

Since p-cells are disjoint, we have for the integrals

$$\int_{C_{(p)}} a^{(p)} = \int_{\sum_{i=1}^{n_p} m_{(p),i} c_{(p),i}} a^{(p)} = \sum_{i=1}^{n_p} m_{(p),i} \int_{c_{(p),i}} a^{(p)}.$$

So the reduction operator is completely determined by integration over all individual p-cells.

Example 1. Let $\Omega = [a, b]$ and let the cell-complex consist of five 0-cells distributed uniformely over the interval as in Figure 4. Let $a^{(0)}(x)$ be a zero form defined on Ω, then $\mathcal{R}a^{(0)}$ gives the 0-cochain

$$C^{(0)} = \sum_{i=1}^{5} a^{(0)}(P_i) c_i^{(0)},$$

where $a^{(0)}(P_i)$ is the evaluation of $a^{(0)}(x)$ in the points P_i. Similarly, let $b^{(1)}(x)$ be a 1-form defined on Ω, then the reduction operator maps $b^{(1)}$ to the 1-cochain

$$C^{(1)} = \sum_{i=1}^{4} \left[\int_{L_i} b^{(1)} \right] c_i^{(1)}.$$

A special case is the 1-form $da^{(0)}(x)$, the exterior derivative of a 0-form, which gives

$$\begin{aligned} C^{(1)} &= \sum_{i=1}^{4} \left[\int_{L_i} da^{(0)} \right] c_i^{(1)} \\ &= \sum_{i=1}^{4} \left[\int_{\partial L_i} a^{(0)} \right] c_i^{(1)} \\ &= \sum_{i=1}^{4} \left[a^{(0)}(P_{i+1}) - a^{(0)}(P_i) \right] c_i^{(1)} \\ &= \delta \sum_{i=1}^{5} a^{(0)}(P_i) c_i^{(0)} = \delta C^0. \end{aligned} \tag{77}$$

This simple example demonstrates that

$$\mathcal{R} \circ d = \delta \circ \mathcal{R}. \tag{78}$$

So taking the exterior derivative at the continuous level and discretizing (reduction) is the same as first discretizing and then applying the coboundary operator. This is true for any differential forms and, therefore, the following diagram commutes.

$$\begin{array}{ccc} \Lambda^k(\Omega) & \xrightarrow{d} & \Lambda^{k+1} \\ \downarrow \mathcal{R} & & \downarrow \mathcal{R} \\ C^{(k)} & \xrightarrow{\delta} & C^{(k+1)} \end{array} \tag{79}$$

Note that the discrete values obtained from the reduction operation are *only point values* for 0-forms. For general p-forms the discrete values will be *integral values*.

5.2. The Reconstruction Operator

The reconstruction operator, $\mathcal{I}$, maps p-cochains onto differential p-forms in such a way that reduction of the reconstructed p-forms give the original cochains, i.e.

$$\mathcal{R} \circ \mathcal{I} = I, \tag{80}$$

where I is the identity operator. We want the reconstruction operator to commute with the exterior derivative and the coboundary operator

$$\mathcal{I} \circ \delta = d \circ \mathcal{I}. \tag{81}$$

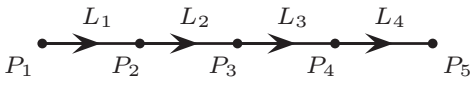

FIG. 4. One dimensional cell-complex covering the interval $[a, b]$.

The reconstruction operator needs to be linear, that is, for all p-cochains $C^{(p)}$ and $D^{(p)}$ defined on the same cell complex K and all $\alpha,\ \beta \in \mathbb{R}$,

$$\mathcal{I}\left(\alpha C^{(p)} + \beta D^{(p)}\right) = \alpha\mathcal{I}\left(C^{(p)}\right) + \beta\mathcal{I}\left(D^{(p)}\right). \tag{82}$$

Finally, we impose an approximation property that $\mathcal{I} \circ \mathcal{R}$ is close to the identity I, i.e., $\mathcal{I} \circ \mathcal{R} = I + \mathcal{O}(h^{\alpha})$, where h denotes the characteristic size of the p-chains and α denotes the order of the reconstruction. In this section, α is arbitrarily high for sufficiently smooth differential forms.

Example 2. Let the 0-chain on the interval $[a, b]$ be as given in Example 1.. Let $h_i(x)$ be the Lagrange interpolant through the points P_i, i.e., $h_i(x)$ is a polynomial of degree $n_p - 1$ such that

$$h_i(P_j) = \begin{cases} 1 & \text{if} \quad i = j \\ 0 & \text{if} \quad i \neq j \end{cases}. \tag{83}$$

The reconstruction of a 0-cochain

$$c^{(0)} = \sum_{i=1}^{n_p} a_i c_i^{(0)}, \tag{84}$$

is then given by

$$a_h^{(0)}(x) = \mathcal{I}(c^{(0)}) = \sum_{i=1}^{n_p} a_i h_i(x), \tag{85}$$

which is just the higher order nodal interpolation of the values a_i defined at the points P_i. Note that the reduction of (85) gives the original 0-cochain given by (84).

The reconstruction of 1-cochains is less straightforward, see [33]. Suppose we can develop basis functions, $e_i(x)$, which satisfy

$$\int_{L_j} e_i(x) = \begin{cases} 1 & \text{if} \quad i = j \\ 0 & \text{if} \quad i \neq j \end{cases}, \tag{86}$$

then the 1-cochain given by

$$c^{(1)} = \sum_{i=1}^{n_l} b_i c_i^{(1)}, \tag{87}$$

gives

$$b_h^{(1)}(x) = \mathcal{I}\left(c^{(1)}\right) = \sum_{i=1}^{n_l} b_i e_i(x). \tag{88}$$

Then reduction to the 1-chain $\sum_{j=1}^{n_l} c_{(1),j}$ gives

$$\begin{aligned} \mathcal{R}\mathcal{I}\left(c^{(1)}\right) &= \mathcal{R}\left[\sum_{i=1}^{n_l} b_i e_i(x)\right] \\ &= \sum_{i=1}^{n_l} b_i \mathcal{R}\left[e_i(x)\right] \\ &= \sum_{i=1}^{n_l} b_i \sum_{j=1}^{n_l}\left[\int_{L_j} e_i(x)\right] c_j^{(1)} \\ &= \sum_{i=1}^{n_l} b_i c_i^{(1)} \\ &= c^{(1)}, \end{aligned}$$

which shows that $\mathcal{R}\mathcal{I}$ equals the identity on 1-cochains. Basis functions $e_i(x)$, which satisfy (86), were derived in [33, 34] and are explicitly given in terms of the nodal Lagrange basis functions $h_i(x)$ by

$$e_i(x) = -\sum_{k=0}^{i-1} dh_k(x), \tag{89}$$

where $dh_k(x)$ is the exterior derivative applied to the 0-forms $h_k(x)$ defined by (83). An example of an edge function is shown in Figure 5. It is straightforward to show that the reconstruction operators given for 0-cochains and 1-cochains are linear and commute with exterior derivative and coboundary operator.

If a reconstructed 1-form is given by

$$a_h^{(0)}(x) = \sum_{i=1}^{n_p} a_i h_i(x), \tag{90}$$

then the exterior derivative $a_h^{(0)}(x)$ is given by

$$\begin{aligned} da_h^{(0)}(x) &= d\sum_{i=1}^{n_p} a_i h_i(x) \\ &= \sum_{i=1}^{n_p} a_i dh_i(x) \\ &= \sum_{i=1}^{n_p} a_i \left[\sum_{k=1}^{i} dh_k(x) - \sum_{k=1}^{i-1} dh_k(x)\right] \\ &= \sum_{i=1}^{n_p} a_i \left[-e_{i+1}(x) + e_i(x)\right] \\ &= \sum_{i=1}^{n_l} (a_{i+1} - a_i)\, e_i(x) \\ &= \sum_{i=1}^{n_l} (\delta a_i)\, e_i(x), \end{aligned} \tag{91}$$

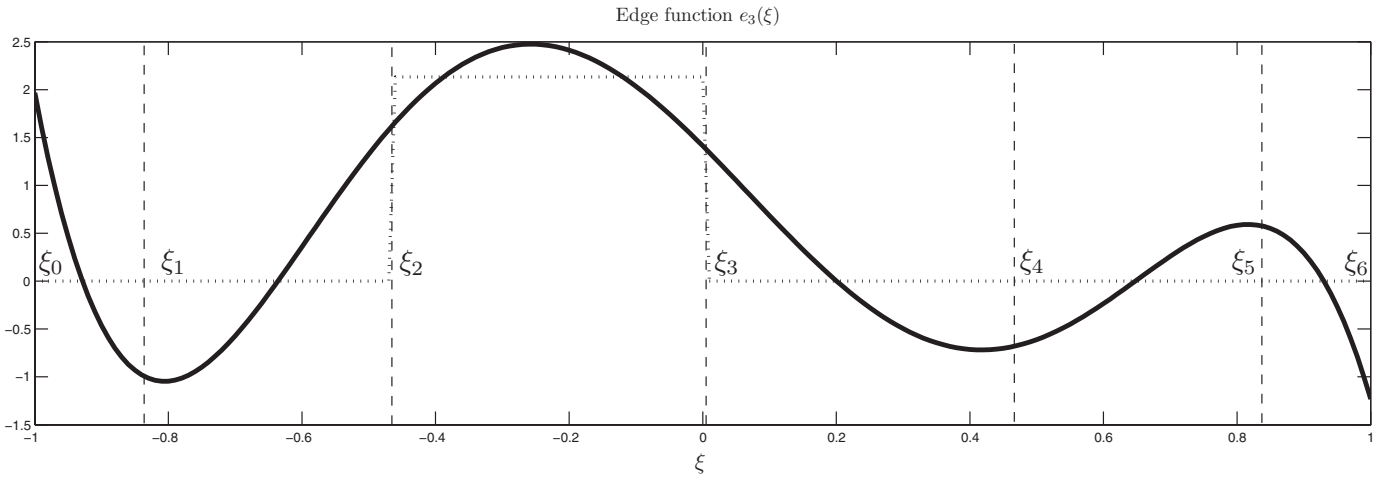

FIG. 5. The edge function $e_3(x)$ of polynomial degree 5. The integral over the interval $[\xi_{i-1}, \xi_i]$ vanishes except for $i = 3$ where the integral evaluates to one.

where we used that

$$e_1(x) = -\sum_{k=1}^{0} dh_k(x) = 0 \quad \text{and} \quad e_{n_p+1} = -\sum_{k=1}^{n_p} dh_k(x)$$
$$= -d \circ \sum_{k=1}^{n_p} h_k(x) = -d \circ 1 = 0.$$

This equation shows that indeed we have that $d \circ \mathcal{I} = \mathcal{I} \circ \delta$.

5.3. The Discrete Hodge Operator

Let $b_h^{(1)}(x)$ be a discrete 1-form given by

$$b_h^{(1)}(x) = \sum_{i=1}^{n_l} b_i e_i(x). \tag{92}$$

Since the Hodge-$\star$ operator is linear we have

$$\star b_h^{(1)}(x) = \sum_{i=1}^{n_l} b_i \star e_i(x) = \sum_{i=1}^{n_l} b_i \epsilon_i(x), \tag{93}$$

where

$$e_i(x) = \epsilon_i(x)\, dx \quad \Longrightarrow \quad \star e_i(x) = \epsilon_i(x) \star dx = \epsilon_i(x).$$

At the end of section 4, we argued that the Hodge-$\star$ operator connects variables defined on dual cell-complexes. In this particular one dimensional case, we can associate with each line segment on the primal complex a point on the dual complex. This situation is depicted in Figure 6. With each line segment on the primal complex, i.e., the line segment between two consecutive black dots is a white dot on the dual complex. With the dual 0-cells (points), we can associate Lagrange polynomials $\tilde{h}_i(x)$ with the property that

$$\tilde{h}_i(\tilde{P}_j) = \delta_{ij}.$$

We can now expand $\star b_h^{(1)}(x)$ as given in (93) in terms of the nodal functions $\tilde{h}_i(x)$ on the dual complex

$$\star b_h^{(1)}(x) = \sum_{j=1}^{\tilde{n}_P} \left[\sum_{i=1}^{n_l} b_i \epsilon_i(\tilde{P}_j) \right] \tilde{h}_j(x). \tag{94}$$

Since $\tilde{n}_p = n_l$ by construction of the dual complex, $\epsilon_i(\tilde{P}_j)$ is square invertible matrix. If we apply the Hodge operator to (94)

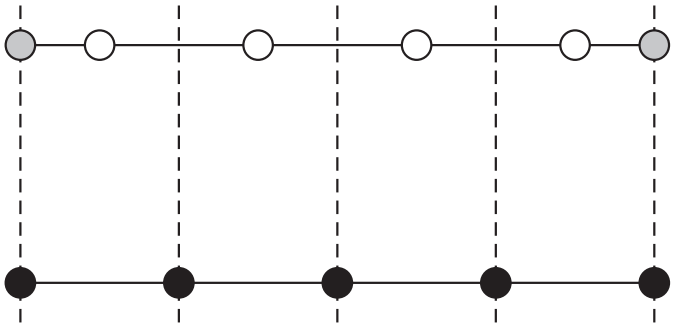

FIG. 6. One-dimensional cell-complex K and its dual complex $\tilde{K}$. The black dots are the 0-cells on the primal complex and the white dots are the 0-cells on the dual complex. The gray dots at the boundary of the dual cell complex are only needed to construct the dual edge functions.

we obtain

$$\begin{aligned}
\star\star b_h^{(1)}(x) &= \star \sum_{j=1}^{\tilde{n}_P} \left[\sum_{i=1}^{n_l} b_i \epsilon_i(\tilde{P}_j) \right] \tilde{h}_j(x) \\
&= \sum_{j=1}^{\tilde{n}_P} \left[\sum_{i=1}^{n_l} b_i \epsilon_i(\tilde{P}_j) \right] \star \tilde{h}_j(x) \\
&= \sum_{j=1}^{\tilde{n}_P} \left[\sum_{i=1}^{n_l} b_i \epsilon_i(\tilde{P}_j) \right] \tilde{h}_j(x)\, dx \\
&= \sum_{k=1}^{n_l} \left[\sum_{j=1}^{\tilde{n}_p} \sum_{i=1}^{n_l} b_i \epsilon_i(\tilde{P}_j) \int_{c_{(1),k}} \tilde{h}_j(x)\, dx \right] e_k(x) \\
&= \sum_{i=1}^{n_l} b_i e_i(x) \\
&= b_h^{(1)}(x),
\end{aligned}$$

where we use the fact that

$$\sum_{j=1}^{\tilde{n}_p} \epsilon_i(\tilde{P}_j) \int_{c_{(1),k}} \tilde{h}_j(x)\, dx = \delta_{ik}.$$

This confirms (57) in the discrete setting.

For a 0-form on the dual complex, we use the white dots on the dual complex in Figure 6. The edge functions on the dual complex are defined slightly differently: In order to define the edge functions on the dual complex we set up Lagrange functions for the dual points, including the gray points in Figure 6. These Lagrange polynomials will be of polynomial degree $\tilde{n}_p + 1$. With these extended Lagrange functions, $\bar{h}_i(x)$, we set up the edge functions on the dual complex by

$$\tilde{e}_i(x) = -\sum_{k=0}^{i-1} \bar{h}_k(x). \tag{95}$$

The reason we use this modification on the dual complex is a result of the fact that on the dual complex not all 1-cells (line segments) are bounded by two 0-cells (points) as can be seen for the first and the last 1-cell in Figure 6. What we in fact do, is set the 0-form on the dual complex to zero in the gray points. This can always be done without loss of generality and in PDE's this will only lead to a modification of the right hand side function.

So any 1-form on the dual mesh can be expanded in terms of the dual edge functions (95)

$$\tilde{b}_h^{(1)}(x) = \sum_{i=1}^{\tilde{n}_l} \tilde{b}_i \tilde{e}_i(x). \tag{96}$$

Application of the Hodge-$\star$ operator and then writing the result in terms of Lagrange functions on the primal grid gives

$$\begin{aligned}
\star\tilde{b}_h^{(1)}(x) &= \star \sum_{i=1}^{\tilde{n}_l} \tilde{b}_i \tilde{e}_i(x) \\
&= \sum_{i=1}^{\tilde{n}_l} \tilde{b}_i \tilde{\epsilon}_i(x) \\
&= \sum_{j=1}^{n_p} \left[\sum_{i=1}^{\tilde{n}_l} \tilde{b}_i \tilde{\epsilon}(P_j) \right] h_j(x).
\end{aligned} \tag{97}$$

Note that the matrices $\epsilon_i(\tilde{P}_j)$, $\tilde{\epsilon}(P_j)$ and their inverses in combination with the exact Hodge-$\star$ operator constitute the discrete Hodge-$\star$ operator $\star^h$ given in (75). This discrete operator depends explicitly on the location of the grid points and the polynomial degree and, therefore, encodes the metric part in any differential model.

In this one-dimensional example, nodal function $h_i(x)$ and edge functions $e_i(x)$ and their counterparts on the dual complex, are the main ingredients for the reconstruction operator $\mathcal{I}$. They should be applied wisely, because nodal recontruction of a 1-cochain or edge interpolation of 0-cochain will lead to erroneous results.

5.4. Multidimensional Discretization

In the previous subsections, differential forms in one dimension were discussed, but these one-dimensional building blocks enable us to set up higher dimensional discretizations by means of tensor products. In the three dimensional case, a zero form can be represented on the primal complex by

$$T_h^{(0)}(x, y, z) = \sum_{i=1}^{n_{p_x}} \sum_{j=1}^{n_{p_y}} \sum_{k=1}^{n_{p_z}} T_{i,j,k} h_i(x) h) j(y) h_k(z). \tag{98}$$

A flux on the primal complex can be represented by

$$\begin{aligned}
q_h^{(2)}(x, y, z) = &\sum_{i=1}^{n_{p_x}} \sum_{j=1}^{n_{l_y}} \sum_{k=1}^{n_{l_z}} q_{i,j,k}^x h_i(x) e_j(y) e_k(z) \\
&+ \sum_{i=1}^{n_{l_x}} \sum_{j=1}^{n_{p_y}} \sum_{k=1}^{n_{l_z}} q_{i,j,k}^y e_i(x) h_j(y) e_k(z) \\
&+ \sum_{i=1}^{n_{l_x}} \sum_{j=1}^{n_{l_y}} \sum_{k=1}^{n_{p_z}} q_{i,j,k}^z e_i(x) e_j(y) h_k(z).
\end{aligned} \tag{99}$$

Note that in this expression, the numbers $q_{i,j,k}^x$, $q_{i,j,k}^y$, and $q_{i,j,k}^z$ are not mere expansion coefficients with respect to a given polynomial basis, but they are the 2-cochains associated with the surfaces on the primal complex and these 2-cochains represent the integral of a continuous flux vector over these surfaces. So they have actual physical meaning.

A 3-form $f^{(3)}$ will be represented by

$$f_h^{(3)}(x, y, z) = \sum_{i=1}^{n_{l_x}} \sum_{j=1}^{n_{l_y}} \sum_{k=1}^{n_{l_z}} f_{i,j,k} e_i(x) e_j(y) e_k(z). \qquad (100)$$

Now suppose that we want to discretize the conservation law $dq^{(2)} = f^{(3)}$, then we should apply the exterior derivative to (99) and equate the result to (100). The exterior derivative of (99), where we use (77) and the fact that the exterior derivative of an edge function is zero ($de_i(x) \equiv 0$), gives

$$dq_h^{(2)}(x, y, z) = \sum_{i=1}^{n_{l_x}} \sum_{j=1}^{n_{l_y}} \sum_{k=1}^{n_{l_z}} \Big[q^x_{i+1,j,k} - q^x_{i,j,k} + q^y_{i,j+1,k} - q^y_{i,j,k} + q^z_{i,j,k+1} - q^z_{i,j,k} \Big] e_i(x) e_j(y) e_k(z). \qquad (101)$$

Note that this expression is written with respect to the same basis functions as the discrete 3-form (100). Therefore, the discrete version of $dq^{(2)} = f^{(3)}$ becomes

$$\sum_{i=1}^{n_{l_x}} \sum_{j=1}^{n_{l_y}} \sum_{k=1}^{n_{l_z}} \Big[q^x_{i+1,j,k} - q^x_{i,j,k} + q^y_{i,j+1,k} - q^y_{i,j,k} + q^z_{i,j,k+1} - q^z_{i,j,k} - f_{i,j,k} \Big] e_i(x) e_j(y) e_k(z) = 0. \qquad (102)$$

Since all basis functions e_i are linearly independent, this equation reduces to

$$q^x_{i+1,j,k} - q^x_{i,j,k} + q^y_{i,j+1,k} - q^y_{i,j,k} + q^z_{i,j,k+1} - q^z_{i,j,k} - f_{i,j,k} = 0 \; \forall i, j, k = 1, \ldots, n_l. \qquad (103)$$

There all several points to make now, which in my view, justifies the use of mimetic methods:

- Equation (103) can also be written as

$$\delta q^{(2)} = f^{(3)},$$

where δ is the coboundary operator, $q^{(2)}$ a 2-cochain on the primal complex and $f^{(3)}$ a 3-cochain on the primal complex. So this equation is purely topological and will always hold, no matter what the shape of the mesh is.
- Equation (103) is independent of the basis functions. So the same expression will be found for low second-order methods (linear basis functions) as for for very high order approximations.
- Suppose we have a mapping Φ from the unit cube Ω' to very distorted domain Ω, then we transform the equation back to the unit cube by means of the pull-back operator Φ^*. The pullback operator acts on the basis functions, but the final result will be independent of the basis functions, therefore, the conservation law will also hold on the very distorted domain. This again shows that this equation is purely topological and independent of the basis functions.
- Equation (103) is exact. The residual is always zero.

The next observation is more generally true and deserves the status of proposition:

Proposition 3. Any physical relation always needs to be written with respect to the same basis functions, just like in (102) and, therefore, the basis functions cancel from the equation. In some cases, this discrete equation contains matrices that depend on the basis functions, for instance, when a discrete Hodge-$\star$ operator is involved, which connects the two dual complexes, but there will be no explicit dependence on functions of x, y, and z anymore.

The exactness and independence of metric for the divergence equation just shown, also holds for relations involving the gradient or the curl operator. For instance, for potential flow problems, we know that the velocity is the gradient of a potential – $u^{(1)} = d\phi^{(0)}$ –, or the definition of vorticity is the curl of the velocity field – $\xi^{(2)} = du^{(1)}$. These relations are all topological and can always be discretized independent of the basis functions. Since $d \circ d \equiv 0$, the two definitions above and the exactness of the discretizations immediately imply that the discrete potential flow will be irrotational. For more challenging

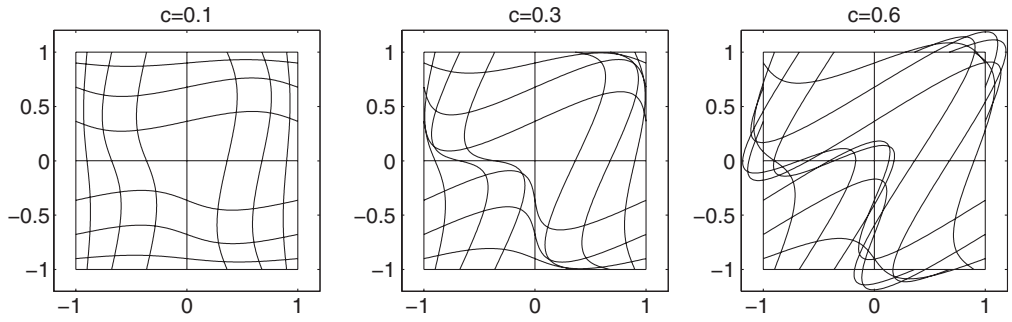

FIG. 7. Three curved grids.

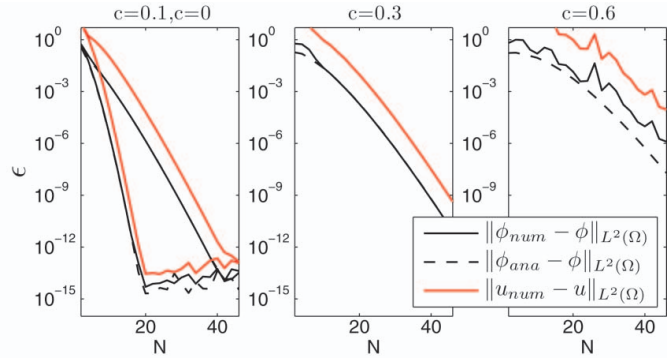

FIG. 8. Convergence on one spectral element as a function of the polynomial degree on the meshes shown in Figure 7. (Color figure available online.)

physical models, this will no longer be the case, but we can then dissect this more complex physical model in parts that can be exactly represented and those parts where approximations are required.

In order to show the performance/robustness of the discretization described in this article, I will present a few examples:

Example 4. The first example is the 2D Poisson equation (52–53) introduced in section 3.6. in curvilinear coordinates, which will demonstrate that the topological equation is exactly satisfied no matter how pathological the mesh is. This test problem is described in more detail in [39], which is based on a similar analysis on orthogonal grids described in [35, 36].

For the calculation of the cochains on cell complexes, the reduction operator $\mathcal{R}$ is required, which consists of integration of a differential k-form over a k-chain. Now suppose that all k-chains are curved and non-orthogonal in the domain Ω. Let Φ be a map from the unit square, Ω' to the curved domain Ω, then we can use the pullback operator to convert k-forms in Ω to k-forms in Ω', using

$$\int_{\Phi(\Omega')} a^{(k)} = \int_{\Omega'} \Phi^* a^{(k)}. \tag{104}$$

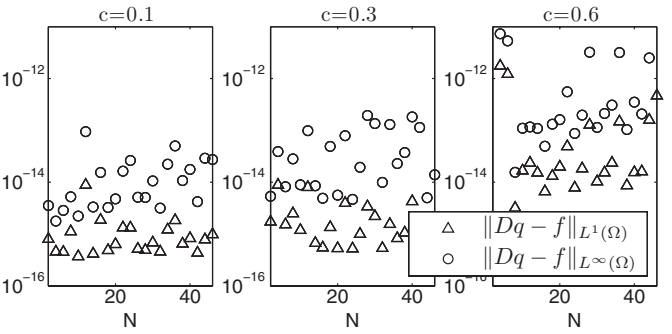

FIG. 9. Residuals of the equation $dq^{(1)} = f^{(2)}$ measured in the L^1- and L^∞-norm for the curved grids shown in Figure 7.

So the equation $dq^{(1)} = f^{(2)}$ on Ω can be written as $\Phi^* dq^{(1)} = \Phi^* f^{(2)}$ on Ω'. But, since the pullback operator and the exterior derivative commute, we have $d(\Phi^* q^{(1)}) = \Phi^* f^{(2)}$. The same holds for the relation $u^{(1)} = d\phi^{(0)}$ on Ω, which gives $\Phi^* u^{(1)} = d(\Phi^* \phi^{(0)})$ on Ω'. The relation $q^{(1)} = \star u^{(1)}$ in Ω can be recast in Ω' by premultiplication by Φ^*

$$\Phi^* q^{(1)} = \Phi^* \star \left(\Phi^*\right)^{-1} \Phi^* u^{(1)}.$$

Now if we introduce the new variables $\bar{\phi}^{(0)} = \Phi^* \phi^{(0)}$, $\bar{u}^{(1)} = \Phi^* u^{(1)}$, $\bar{q}^{(1)} = \Phi^* q^{(1)}$, and $\bar{f}^{(2)} = \Phi^* f^{(2)}$, then the governing equations in Ω' are given by

$$d\bar{\phi}^{(0)} = \bar{u}^{(1)}, \quad d\bar{q}^{(1)} = \bar{f}^{(2)}, \quad \bar{q}^{(1)} = \bar{\star}\bar{u}^{(1)}, \tag{105}$$

where $\bar{\star} = \Phi^* \star (\Phi^*)^{-1}$. So the curvilinear problem can be reformulated as a problem in orthogonal coordinates and the only thing that changes is the Hodge-$\star$ operator in Ω'. In Figure 7, three meshes are shown and as a test problem we will solve the Poisson equation with

$$f^{(2)}(x, y) = -2\pi^2 \sin(\pi x) \sin(\pi y),$$

and we impose homogeneous Dirichlet boundary conditions. The curved grids in Figure 7 are generated by

$$x(\xi, \eta) = \xi + c \sin(\pi\xi) \sin(\pi\eta), \tag{106}$$

$$y(\xi, \eta) = \eta + c \sin(\pi\xi) \sin(\pi\eta).$$

The convergence results on these three meshes are shown in Figure 8. The solid black line is the convergence of ϕ, the dashed black line is the interpolation error when the exact solution is interpolated on the curved grids, and the gray line shows the convergence rate of u. It can be noted that when the grids are curved, but non-selfoverlapping, exponential convergence

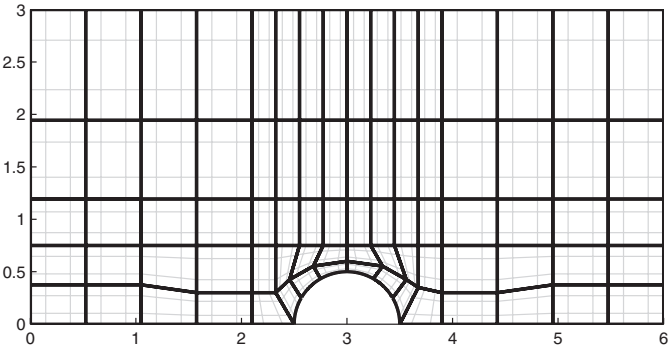

FIG. 10. Spectral element mesh used for the potential flow over a cylinder consisting of 80 elements.

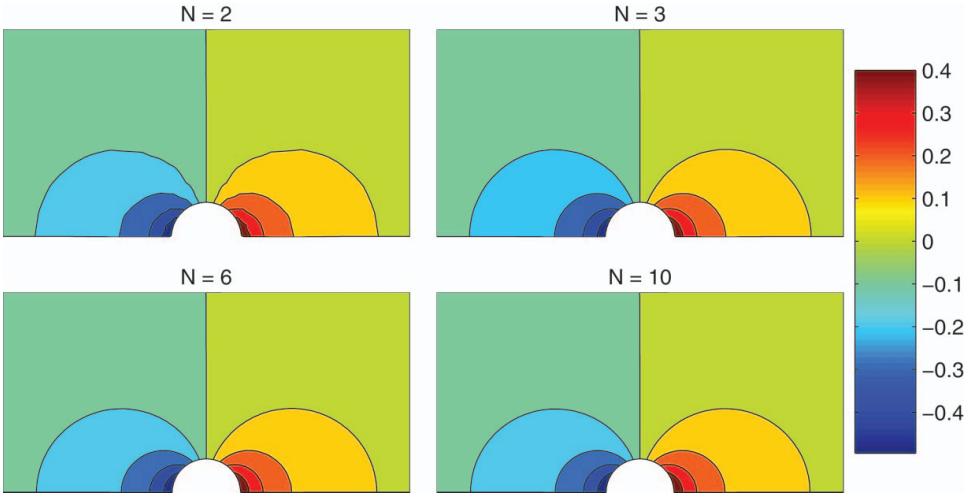

FIG. 11. Plots of the disturbance potential for $N = 2$, $N = 4$, $N = 6$ and $N = 10$. (Color figure available online.)

with the polynomial degree is observed and the numerical discretization error equals the interpolation error. In the case of a self-overlapping grid, convergence is much more irregular and the discretization error is larger than the interpolation error. But, despite the irregular convergence, the error decreases with polynomial enrichment, showing the robustness of the proposed method. We claimed at the beginning of this section, that the conservation equation $dq^{(1)} = f^{(2)}$ only depends on the topology of the mesh and not on the actual shape of the mesh. In Figure 9, these residuals are measured in the L^1-norm and the L^∞-norm given by

$$\|a\|_{L^1(\Omega} = \int_\Omega |a|\, d\Omega \quad \text{and} \quad \|a\|_{L^\infty(\Omega)} = \sup |a|.$$

Figure 9 shows that the discrete equations $dq_h^{(1)} = f^{(2)}$ is satisfied up to machine precision on all three grids.

Example 5. This next example concerns a steady, irrotational, incompressible, inviscid flow over a circular cylinder in the absense of body forces, taken from [37]. This is an application using multiple elements. We will only model half the domain for which the mesh is shown in Figure 10. Since this domain is contractible, the Poincaré lemma tells us that when the flow is irrotational, i.e., $du^{(1)} = 0$, there exists a $\phi^{(0)}$ such that $u^{(1)} = d\phi^{(0)}$. Conservation of mass is given by $dq^{(1)} = 0$, with $q^{(1)} = \star u^{(1)}$. For this problem, the exact solution is analytically known, so the exact boundary conditions are prescribed. On the symmetry plane and the cylinder the flux is set to zero. At the remainder of the boundary, the potential is prescribed. Results for various polynomial degrees are shown in Figure 11. The cylinder is generated by a transfinite mapping. The results in Figure 11 are almost indistinguishable for $N \geq 4$. The convergence of the discrete velocity field $u_h^{(1)}$ to the exact velocity field $u^{(1)}$ in the L^2-norm is given in Figure 12. This figure displays a straight line in a semi-log plot, which indicates exponential convergenve towards the exact solution. Conservation of mass $dq_h^{(1)} = 0$ is satisfied up to machine precision for all polynomial degrees.

Note that in Example 4. and Example 5. we consider the scalar Laplace equation, i.e., the Laplace equation for 0-forms. With the techniques developed in this article, we can extend this to more general Laplace operators. The Poisson equation for differential forms is given by

$$\Delta a^{(k)} := (\star d \star + d)^2\, a^{(k)} = (\star d \star d + d \star d \star)\, a^{(k)} = f^{(k)}, \tag{107}$$

which in the case $k = 0$ reduces to

$$\Delta a^{(0)} = \star d \star d a^{(0)} = f^{(0)}, \tag{108}$$

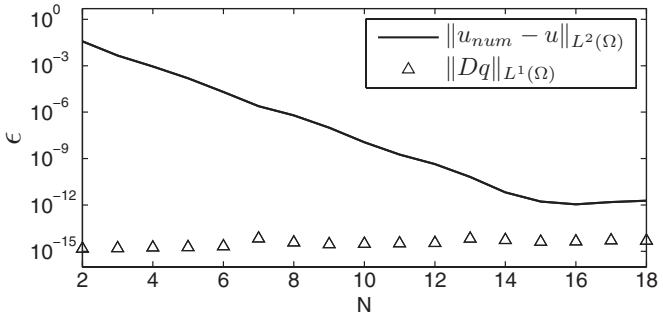

FIG. 12. Convergence of the error in the fluid velocity in the L^2-norm and the norm of the incompressibility constraint in the L^1-norm.

and for $k = n$ is given by

$$\Delta a^{(n)} = d \star d \star a^{(n)} = f^{(n)}. \tag{109}$$

6. FINAL REMARKS

As the title of this article suggests, this is only an introduction into mimetic techniques and we restricted ourselves to elliptic problems. We merely scratched the surface, but already with these tools some real world applications can be solved. For time-dependent problems, the time domain has to be discretized also. Mattiussi [2] gives the general structure when time becomes an independent variable as well. If we want to solve hyperbolic problems, we need to extend our machinery with the interior product between differential forms and vector fields. With the exterior derivative discussed in this article and the interior product, we can set up the Lie derivative for all k-forms. So wave phenomena in fluids and solids and associated boundary conditions fall into the framework of mimetic methods, but are beyond the scope of this article. We will report on this in future papers.

In order to extend the applicability of the methods proposed in this article, many concepts require a much more formal definition and many of the statements in this article need much more rigorous proofs. This will be done in the paper by Kreeft et al. [38], which will be submitted shortly.

I hope that this short introduction has elucidated what we mean when we talk about compatible or mimetic discretization techniques. The grid that we generally employ in numerical calculations is an integral part of the description of physics and the basic functions that we use should interpolate the intergal quantities in the first place. That this is not only the case for the simple problems given in this article can be seen in the forthcoming book by Tonti [40], where a plethora of physical theories is organized in so-called classification diagrams.

REFERENCES

1. E. Tonti, On the mathematical structure of a large class of physical theories. Accademia Nazionale dei Lincei, estratto dai Rendiconti della Classe di Scienze fisiche, matematiche e naturali, Serie VIII, Vol. LII, fasc. 1, Gennaio, 1972.
2. C. Mattiussi, The finite volume, finite difference, and finite elements methods as numerical methods for physical field problems. In: Advances in Imaging and Electron Physics, vol. 113, pp. 1–146, Elsevier, Amsterdam, 2000.
3. Alain Bossavit's Japanese papers. Available from http://butler.cc.tut.fi/~bossavit/Books/IEEEJapan.html
4. J. Hyman, M. Shaskov, and S. Steinberg, The numerical solution of diffusion problems in strongly heterogeneous non-isotropic materials, J. Comput. Phys., vol. 132, pp. 130–148, 1997.
5. N. Robidoux, A new method of construction of adjoint gradients and divergences on logically rectangular smooth grids. In: Finite Volumes for Complex Applications: Problems and Perspectives, First International Symposium, July 15–18, 1996. F. Benkaldoun and R. Vilsmeier, Éditions Hermès, Rouen, France, pp. 261–272, 1996.
6. N. Robidoux, Numerical solution of the steady diffusion equation with discontinuous coefficients, PhD Thesis, University of New Mexico, Albuquerque, NM, 2002.
7. M. Shashkov, Conservative Finite-Difference Methods on General Grids. CRC Press, Boca Raton, FL, 1996.
8. M. Hyman and S.S. Steinberg, The convergence of mimetic discretization for rough grids, Comput. & Math. Appl. (CAM), vol. 47, nos. 10–11, pp. 1565–1610, 2004.
9. S. Steinberg, A discrete calculus with applications of high-order discretizations to boundary-value problems, Comput. Meth. Appl. Math., vol. 42, no. 4, pp. 228–261, 2004.
10. S.L. Steinberg and J.P. Zingano, Error estimates on arbitrary grids for a 2nd-order mimetic discretization of Sturm-Liouville problems, Comput. Meth. Appl. Math., vol. 9, no. 2, pp. 192–202, 2009.
11. N. Robidoux and S. Steinberg, A discrete vector calculus on tensor grids, Comput. Meth. Appl. Math., vol. 11, no. 1, pp. 23–66, 2011.
12. P.B. Bochev, A discourse on variational and geometric aspects of stability of discretizations. In: 33rd Computational Fluid Dynamics Lecture Series, VKI LS 2003–05, H. Deconinck, Ed., ISSN0377-8312. Von Karman Institute for Fluid Dynamics, Rhode Saint Genese, Belgium, 2005.
13. P.B. Bochev and J.M. Hyman, Principles of mimetic discretizations of differential equations. In: IMA Volume 142, D. Arnold, P. Bochev, R. Lehoucq, R. Nicolaides, and M. Shashkov, Eds., Springer Verlag, Berlin, 2006.
14. D. Arnold, R. Falk, and R. Winther, Finite element exterior calculus, homological techniques and applications, Acta Numer., vol. 15, pp. 1–155, 2006.
15. D. Arnold, R. Falk, and R. Winther, Finite element exterior calculus: From Hodge theory to numerical stability, AMS, vol. 27, no. 2, pp. 281–354, 2010.
16. F. Brezzi and A. Buffa, Innovative mimetic discretizations for electromagnetic problems, J. Comput. Appl. Math., vol. 234, pp. 1980–1987, 2010.
17. R. Hiptmair, Discrete hodge operators. Numer. Math. vol. 90, pp. 265–289, 2001.
18. T. Tarhasaari, L. Kettunen, and A. Bossavit, Some realizations of the discrete Hodge operator: A re-interpretation of finite element techniques. IEEE Trans. Magnetics, vol. 35, no. 3, pp. 1494–1497, 1999.
19. B. Perot, Conservation properties of unstructured staggered mesh schemes, J. Comput. Phys. vol. 159, no. 1, pp. 58–89, 2000.
20. B. Perot, Discrete conservation properties of unstructured mesh schemes, Annu. Rev. Fluid Mech, vol. 43, pp. 299–318, 2011.
21. X. Zhang, D. Schmidt, and B. Perot, Accuracy and conservation properties of a three-dimensional unstructured staggered mesh scheme for fluid dynamics, J. Comput. Phys., vol. 175, no. 2, pp. 764–791, 2002.
22. M. Desbrun, A.N. Hirani, M. Leok, and J.E. Marsden, Discrete Exterior Calculus. E-print arXiv:math/0508341v2 [math.DG] on arxiv.org, 2005.
23. M. Desbrun, E. Kanso, and Y. Tong, Discrete differential forms for computational modeling. ACM SIGGRAPH ASIA 2008 Courses, SIGGRAPH Asia'08; Singapore; December 10–13, 2008.
24. J.D. Anderson Jr., Fundamentals of Aerodynamics, 4th Ed. McGraw-Hill Science, Boston, MA, USA, 2005. ISBN 0072950463.
25. H. Flanders, Differential Forms with Applications to the Physical Sciences. Academic Press, Inc., New York, 1963.
26. C.W. Misner, K.S. Thorne, and J.A. Wheeler, Gravitation, 2nd Ed. W. H. Freeman, New York, 1973.
27. M. Spivak, Calculus on Manifolds: A Modern Approach to Classical Theorems of Advanced Calculus. HarperCollins, New York, 1971. ISBN 0805390219.
28. J.E. Marsden and T.J.R. Hughes, Mathematical Foundations of Elasticity. Prentice Hall, Inc., Englewood Cliffs, NJ, USA, 1983.
29. W.S. Massey, Singular Homology Theory. In: Graduate Texts in Mathematics, vol. 127, 1st Ed., 1991. Corr. 3rd printing, 1980. ISBN: 978-0-387-97430-9.
30. I.M. Singer and J.A. Thorpe, Lecture Notes on Elementary Topology and Geometry. Springer, Berlin, Reprint, 1976.

31. H. Whitney, Geometric Integration. Dover Publications, New York, 2000.
32. J. Dieudonné, A History of Algebraic and Differential Topology, 1900–1960. pps. 1–648, Birkhäuser, Boston, MA, USA, 1989.
33. M.I. Gerritsma, Edge functions for spectral element methods. In: Spectral and High Order Methods for Partial Differential Equations, J.S. Hesthaven and E.M. Rønquist, Eds., Lecture Notes in Computational Science and Engineering, Springer, Berlin, vol. 76, pp. 199–207, 2010.
34. N. Robidoux, Polynomial histopolation, superconvergent degrees of freedom and pseudospectral discrete Hodge operators. To appear: http://www.cs.laurentian.ca/nrobidoux/prints/super/histogram.pdf, 2008.
35. M.I. Gerritsma, M. Bouman, and A. Palha, Least-squares spectral element method on a staggered grid, 7th International Conference, LSSC 2009, Sozopol, Bulgaria, June 2009. I. Lirkov, S. Margenov, and J. Waśniewski, Eds., Lecture Notes in Computer Science, 5910, Springer, Berlin, pp. 653–661, 2010.
36. A. Palha and M.I. Gerritsma, Mimetic least-squares spectral/*hp* finite element method for the Poisson equation, 7th International Conference, LSSC 2009, Sozopol, Bulgaria, June 2009. I. Lirkov, S. Margenov, and J. Waśniewski, Eds., Lecture Notes in Computer Science, 5910, Springer, pp. 662–670, 2010.
37. M. Bouman, Mimetic spectral element methods for elliptic problems, MSc Thesis, TU Delft, Delft, The Netherlands, 2010.
38. J.J. Kreeft, A. Palha, and M.I. Gerritsma, Mimetic framework on curvilinear quadrilaterals of arbitrary order, Found. Comp. Mat., 2011.
39. M. Bouman, A. Palha, J.J. Kreeft, and M.I. Gerritsma, A conservative spectral element method for curvilinear domains. In: Spectral and High Order Methods for Partial Differential Equations, J.S. Hesthaven and E.M. Rønquist, Eds., Lecture Notes in Computational Science and Engineering, Springer, Heidelberg, vol. 76, pp. 111–119, 2010.
40. E. Tonti, The common structure of physical theories. To appear, Birkhäuser-Springer, 2011.